Evaluation of Toxicity Levels and Cytotoxicity Mechanisms of Corexit 9500

by

Mengyuan Zheng

A thesis submitted to the Graduate Faculty of
Auburn University
in partial fulfillment of the
requirements for the Degree of
Master of Science

Auburn, Alabama
August 3, 2013

Approved by

T. Prabhakar Clement, Co-Chair, Groome Professor of Civil Engineering
Muralikrishnan Dhanasekaran, Co-Chair, Associate Professor of Pharmacy Science
Joel Hayworth, Associate Research Professor of Civil Engineering

Abstract

The 2010 British Petroleum (BP) oil spill in the Gulf of Mexico has raised many ecological and health concerns. BP predominately used Corexit9500A to disperse crude oil in the Gulf of Mexico to prevent shoreline contamination. The use of Corexit is a concern since the impacts of Corexit on human health and environment are unclear. This study attempts to quantify the *in-vitro* toxicity of Corexit by using cell lines from different tissues, and also provides data regarding toxicity mechanisms. The study provides indirect evidence on the effects of Corexit on human health effects. A 3-(4,5-Dimethylthiazol-2-yl)-2,5-diphenyl tetrazolium bromide (MTT) assay was used to study the cytotoxicity effects. Reactive oxygen species (ROS) and lipid peroxidase (LPO) were measured by fluorometric and colorometric methods. Also glutathione (GSH) content and superoxide dismutase (SOD) and catalase activity were measured to develop a better understanding of toxicological pathways. Results show that the LC50 of Corexit in B16/BL6 cells is 16 ppm, in 1321N1 cells is 33 ppm, in H19-7 cells were 70 ppm, in HK-2 cells is 95 ppm, and in HEK-293 cells is 120 ppm. When H19-7 cell were treated with 80 ppm Corexit for 24 hours, ROS increased considerable ($n=6$, $p<0.005$), SOD increased ($n=6$, $p<0.001$), and catalase decreased ($n=6$, $p<0.005$). The imbalance between ROS generation and excretion indicates that the cell underwent oxidative stress, which leads to the cell death; the increase in LPO ($n=6$, $p<0.005$) verifies this assumption.

Acknowledgments

I would like to express my deepest gratitude to my advisor, Dr. T. Prabhakar Clement, for his patience and continuous support without which I would not have achieved my goal. His perseverance in the field of science and engineering has been a tremendous influence.

I would like to thank my committee members, Dr.Muralikrishnan Dhanasekaran for his enlightening comments and useful remarks, and Dr. Joel Hayworth for his encouragement and helpful instructions that guided me through my thesis and manuscript.

In addition, I would like to extend my thanks to Dr. Mark O. Barnett for his tremendous support, both academically and personally, Dr. Raj Amine for his valuable advice and his forgiveness after I broke his multi-channel pipette, Dr. Vishnu Suppiramaniam for motivating me, Dr. Tahir Husani and his research group for their support in assistant me with my experiments and Daniel Gingerich for his editorial assistance with in my thesis and his professional advice.

Furthermore, I would also like to acknowledge the essential role of my co-workers, for their hard working nature, optimistic attitude towards science, and persistent pursuit of their dreams will be something I will always remember. I would also like to thank my friends here in Auburn and back in China; their friendship and support make my life here complete.

This research was, in part, funded by the Department of Civil Engineering, and by a VPR grant received by Dr. Dhanasekaran and Dr. Clement.

I dedicate this MS thesis to my Mother, for her love and support has been my strength throughout my studies at Auburn University and has been essential for the completion of my thesis.

Table of Contents

List of Tables

List of Figures

CHAPTER 1. Introduction and literature review

1.1 The *Deepwater Horizontal* Oil Spill

The *Deepwater Horizontal* (DWH) oil spill which occurred on April 20th, 2010 was the largest oil spill in US history. The accident was caused by the explosion of the MC252 well located 1500 m deep and 84 km away from Venice, Louisiana (Lubchenco et al., 2012). It took 87 days for the damaged well to be totally shut down. It was estimated that 780 000 m^3 oil was released into the ocean (Graham et al., 2010).

Crude oil is a complex mixture containing thousands of chemicals with a density ranging from 800 to 900 kg/m^3. The density of sea water is approximately 1200 kg/m^3; therefore, raw crude oil will float on sea water (ATSDR, 1999). Crude oil contains several toxic compounds including polycyclic aromatic hydrocarbons (PAHs) which make up about 0.2 to 7% by weight of the oil (NRC, 2003). Several of these PAHs have been identified as environmental toxins and studies have shown that exposure to these compounds poses a considerable risk to human health (Goldstein et al., 2011, Hayworth, 2011).

The adverse effects of an oil spill on local economies can be enormous. For example, in 2008, approximately 2 million tourists visited Alabama's Gulf Coast communities and spent more than 3 billion dollars, sustaining over 59,000 jobs (Hayworth et al., 2011). This massive tourist economy was considerably impacted by the DWH oil spill. Additionally, the coastal environment near the beaches was heavily impacted, placing many animals, such as loggerhead and Kemp Ridley sea turtles (endangered species) and non-game migratory birds at risk

(Hayworth et al., 2011). Previous oil spills, such as, the 1989 *Exon Valdez* oil spill have led to long term chronic ecological health problems, including higher mortality of new born animals and declines in marine animals like fish (salmon fry, Masked Greenling, Crescent Gunnel), sea otters, and sea ducks (Harlequin Duck, Barrow's Goldeneyes).

Three basic approaches are often used to manage oil spills in marine environments (mechanical booms, onsite burning, and dispersant treatment). Mechanical methods, where sorbent booms are placed on the sea surface to prevent oil from spreading away from the source, are limited by the intensity of ocean waves (NRC, 1989). Onsite burning of oil on the sea surfact is often incomplete. Additionaly, burning of oil can cause severe environmental impacts; for example, the incomplete burning of oil can produce carbon monoxid (Bartha and Atlas, 1976). Successful onsite burning requires oil slick thickness to be such that the thickness of the oil slick heavy to support burning (approximately 0.1 mm; (NRC, 1989). Dispersants act to reduce the interfacial tension between water and oil, allowing the oil to break into small globules which are distributed over a larger volumn of water (NRC, 1989). This enhances the removal of oil through volitalizaation, photo-oxidation, and biodegradation (NRC, 2003).

During the DWH oil spill, both government officials and academic scientists were involved in emergency response actions. One of the primary interests of government officials was to quantify the amount of oil discharged from the well, the rate of discharge, and the spatial distribution of oil within the water column and on the sea surface (Lubchenco et al., 2012). By measuring the total flow rate of oil discharging from the well, it was estimated that only about half of the oil discharged from the well reached the surface of the sea. Of this amount, about 5 % of the surface oil was burned, 3 % was skimmed, and 17 % of the oil was directly recovered from the riser pipe (Lehr et al., 2010).

Public media reports regarding the DWH disaster have generally claimed that the bulk concentration of oil in sea water samples fell below background levels approximately 100 days after the MC252 well was capped (Lubchenco et al., 2012). However, wildlife and the aquatic organisms were still at risk of being affected by remnant oil reaching coastal systems long after the discharge of oil from the MC252 well. For example, studies demonstrated increased accumulation of oil on sediment and coral communities around the well head (Lubchenco et al., 2012). From June 2010 to the present, tar balls and tar mat fragments have continuously been deposited on Alabama's beaches. According to the field research completed during September 2012 (following Hurricane Isaac), more than 150 tar balls ranging in size from 1 to 4 cm were collected within a small $20m^2$ control region at an Alabama beach within approximately 15 minutest. (Clement et al., 2012).

Another major concern related to the DWH disaster is the safety of seafood for human consumption, since the Gulf of Mexico provides one-fifth of the sea food consumed in the United States. The potential accumulation of PAHs in seafood is a major concern due to their environmental persistence and toxicity. Previous studies have indicated that both fish and crustaceans have the ability to metabolize PAHs; however, bivalves (oysters, scallops, mussels) do not have this ability (Lubchenco et al., 2012). Therefore, once sea water is contaminated by oil, bivalves in the contaminated area should not be consumed by human (Lubchenco et al., 2012).

The DWH disaster demonstrated that more effective technologies need to be developed to stop the flow of oil from damaged deep sea wells. Also, a greater understanding of the physical and ecological consequences to natural systems likely to be affected by oil spills is needed. Enhanced capacities such as technical experts, well-trained personnel, and better equipment are

needed. Also, regional scientific collaboration networks should be established to provide better communication platforms between multi-disciplinary scientists, while maintaining an intimate engagement between government and industry, to decrease the response time after an oil spill (Lubchenco et al., 2012).

1.2 Dispersant

Although significant efforts have been made in reducing the frequency of oil spills in marine environments, the demand for oil makes the elimination of oil spills impossible. Most mechanical responses to oil spills are limited, and onsite burning has negative environmental consequences. Therefore, in most cases, the use of dispersants is recommended as a potential first response option (NRC, 2003).

Dispersants are a mixture of three types of chemicals: surfactants, additives and solvents. Surfactants are the main components in oil dispersants. Additives increase the degradation ability of dispersants, raise the solubility of dispersants in the oil phase, and enhance the stability of dispersed oil droplets. Solvents enhance the homogenization of surfactants and additives in the dispersant (Clayton et al., 1993). As shown in Figure 1-1, when a dispersant is applied to oil in an aqueous environment, the hydrophilic ends of surfactant monomers are attracted to the aqueous phase, and the hydrophobic ends of surfactant monomers are attracted to the organic oil phase. This results in a reduction in surface tension between the water and oil phases, facilitating the formation of oil-surfactant micelles (Milinkovitch et al., 2012). The critical micelle concentration (CMC) refers to the concentration threshold when surfactants form homogeneous monolayers in the oil phase. When the concentration of surfactants surpasses the CMC, oil-surfactant micelles will form (Clayton et al., 1993). Figure 1-2 shows a typical surfactant

micelle in which a small oil droplet is surrounded by a surfactant monolayer. The ideal diameter for oil-surfactant micelles is less than 1 mm. Once micelles are formed, oil droplets more easily mix in the water column and are less prone to re-aggregate because of the presence of the surfactant monolayer. The efficiency of the dispersant refers to the amount of dispersant required to reach the CMC (Clayton et al., 1993). Although dispersed oil enhances natural degradation processes, it also increases bioavailability to marine organisms as a result of the reduced size of oil droplets. Studies have shown that the decreased oil size can be related to increased toxicity levels (Bobra et al., 1989).

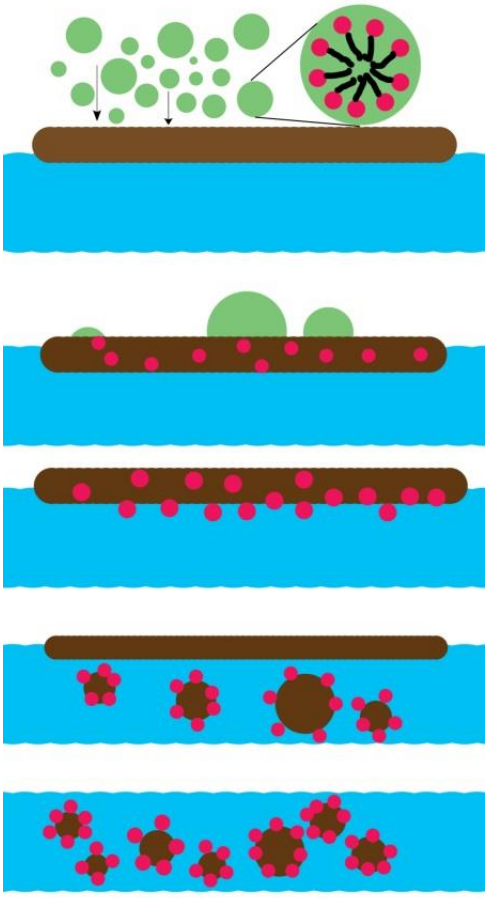

Figure 1-1 Orientation of surfactant molecule oil- water interface (Wikipedia, 2010)

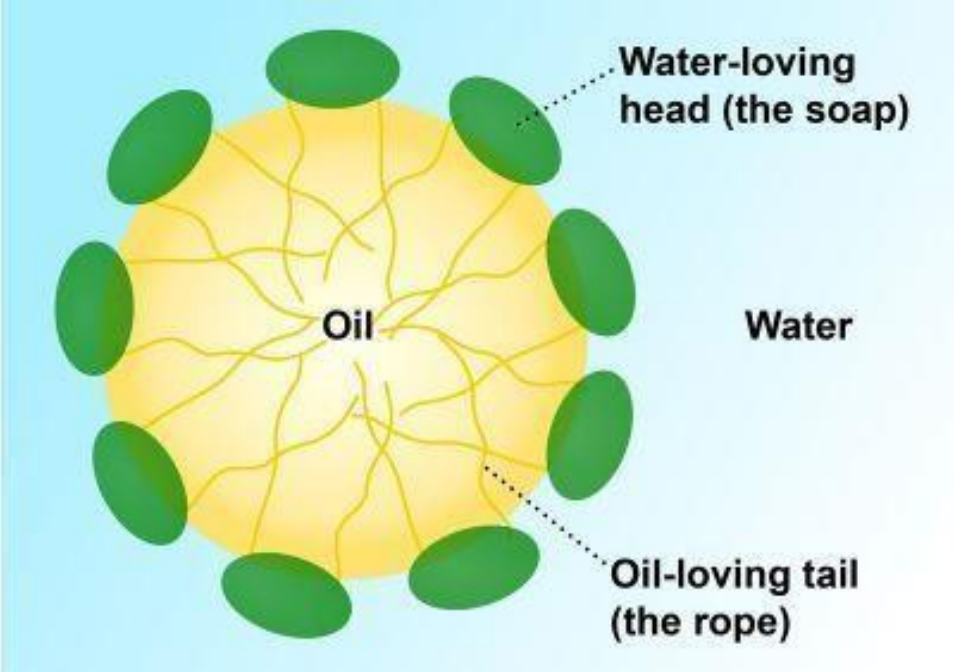

Figure 1-2 Surfactant Micelle (Commer, 2010)

Evaluating the environmental tradeoff s from dispersant use is one of the more difficult decisions for oil spill responders to make. By transferring oil from the surface of the ocean to the larger water column, dispersants protect surface dwelling organisms from exposure to oil; however, they also increases the chances exposure of water column and benthic organisms to toxic oil contaminants (NRC, 2005). The availability of eco-toxicology data to evaluate the potential impacts of dispersants on marine ecosystems is lacking. Particularly, the long term ecological impacts of dispersed oil are not well documented or studied. Countries including France, South Africa, Canada, New Zealand, Norway and the United Kingdom have established standards for deciding whether to use dispersants under specific circumstances. In the United States, there are certain preapproved zones for dispersant application, usually at places 10 meters under the water surface where there is rapid mixing and dilution (NRC, 2005).

Before the application of dispersants, the effectiveness of a dispersant on an oil spill needs to be decided. A suitable dispersant should be selected based on the gravity, viscosity, wax and asphaltene content of the oil (NRC, 1989). The recommended proportion of dispersant to oil ranges from 1:20 to 1:60 (sometimes the ratio can be as high as 1:10 if the oil is more emulsified or possesses a higher viscosity). The ideal partial size of oil-surfactant particles can range from 600 to 1000 microns; small particles may cause an aerosol to be formed, while large particles may pass through the oil layer (NRC, 2005).

Application of dispersants is usually driven by two goals: (1) decreasing the particle size of oil to facilitate the natural biodegradation of the dispersed oil, and (2) protect marine organisms from direct contact with bulk oil (Lubchenco et al., 2012). During the DWH oil spill, dispersants were applied by two methods: surface application by aircraft, and subsea application directly at the wellhead. Subsea application had not been widely used prior to its use during the DWH incident. An argument in favor of subsea application is that the increased exposure of dispersant to oil before oil becomes emulsified on the sea surface decreases the amount of dispersant required, as well as protecting onsite workers from dispersant inhalation (Lubchenco et al., 2012). An argument against the use of dispersants includes potential unknown outcomes; for example, concerns that hypoxia phenomenon may be triggered by dispersed oil (Lubchenco et al., 2012).

During DWH oil spill, dispersants were used in an effort to decrease the interfacial tension and to form smaller oil droplets which could be more easily degraded by bacteria in the water column. Hydrocarbon-utilizing microorganisms can naturally degrade hydrocarbons (Atlas, 1995). Studies have shown that γ-Proteobacteria, an indigenous petroleum degrader,

increased their abundance after the DWH oil spill; this supported the likelihood of enhanced intrinsic bioremediation of DWH oil in the Gulf of Mexico (Hazen et al., 2010).

During the DWH response, approximately 6800 m3 of dispersants were applied at the sea surface and 3000 m3 were applied at the well head (OSTA, 2011). However, deep-water injection of dispersants has never been approved as a response plan by the federal government. Gulf of Mexico residents were concerned about the potential toxicity of dispersants because of health concerns from previous oil spills. In 1967, the Torrey Canyon Spill discharged 20412 m3 of crude oil into the ocean off the southwest coast of the United Kingdom. To disperse the oil floating on the surface, over 9529 m3 of dispersant was applied (Southward and Southward, 1978). It was later found that the oil itself was not very toxic, and that most of the seashore organisms and algae were killed as a result of exposure to the dispersant (Blumer, 1972, Southward and Southward, 1978).

The primary components of the two dispersants used during the DWH oil response, Corexit 9500 and Corexit 9527, are listed in Table 1-1. These two dispersants contained similar components, the major difference is that Corexit 9500 does not contain 2-butoxyethanol (EPA, 2010). The chemical 2 butoxyethanol was suspected of causing human respiratory, nervous system, liver, kidney and blood disorders during the Exxon Valdez oil spill response (Lustgarten, 2010). Due to the toxic nature of 2-butoxyethanol, on May 14th, 2010, the US Environment Protection Agency (EPA) required BP to replace the Corexit 9527 with another less toxic dispersant from the approved list on National Contingency Plan Product Schedule (EPA, 2010).

Two additional components in Corexit 9500 are propylene glycol and dipropylene glycol. Propylene glycol is commonly used in food, drugs, shampoo, mouthwash, and dipropylene glycol is used in cleansers, degreasers, paints, plasticizers (Dickey and Dickhoff, 2011). Organic

sulfonates are synthetic chemicals and act as a surfactant to inhibit oil emulsification and promote oil dispersion into water (NIH, 2013). The type of sulfonates used in both forms of Corexit is dioctyl sodium sulfosuccinate (DOSS). DOSS has been used as flavoring agent in food, and can cause diarrhea and intestinal irritation to rodents when injected orally (Dickey and Dickhoff, 2011). Petroleum distillates in Table 1-1 refer to hydrocarbons containing between 8-20 carbon atoms; the oral toxicity to most organisms of these substances is low. The last three items in Table 1-1 are widely used as wetting agents or as emulsifying agents in several personal care products (Dickey and Dickhoff, 2011).

Table1-1 Components of Corexit9500 and Corexit9527 from EPA

CAS No.	Chemical Name	Corext 9527	Corexit 9500
111-76-2	Ethanol, 2-butoxy-	X	n/a
57-55-6	1,2-Propanediol (Propylene glycol)	X	X
29911-28-2	2-Propanol, 1-(2-butoxy-1-methylethoxy)- (Dipropylene glycol)	X	X
577-11-7	Butanedioic acid, 2-sulfo-, 1,4-bis(2-ethylhexyl) ester, sodium salt (1:1) (DOSS)	X	X
64742-47-8	Distillates (petroleum), hydrotreated light	n/a	X
1338-43-8	Sorbitan, mono-(9Z)-9-octadecenoate (Span 80)	X	X
9005-65-6	Sorbitan, mono-(9Z)-9-octadecenoate, poly(oxy-1,2-ethanediyl) derivs (Tween 80)	X	X
9005-70-3	Sorbitan, tri-(9Z)-9-octadecenoate, poly(oxy-1,2-ethanediyl) derivs (Tween 85)	X	X

After dispersant was applied during DWH oil spill, there was a concern that dissolved oxygen (DO) level in the sea would decrease to hypoxic levels, as a result of dispersed oil droplets stimulating deep-sea indigenous petroleum degraders (Hazen et al., 2010). Continuous monitoring of DO during dispersant application in fact indicated a decreased level of DO in sea water, but these never reached hypoxic levels (JAG, 2012). The particle size of dispersed oil in the DWH oil spill was measured to test the efficiency of dispersant; the results showed the diameter of the dispersed oil droplets ranged from 2.5 μm to 65 μm, in accordance with the expected particle size (JAG, 2010).

To determine whether dispersants used in the DWH response would persist in the environment, both offshore and near-shore water samples were collected for testing of the major constituents in the dispersant (Lubchenco et al., 2012). The components tested included butoxyethanol, dipropylene, glycol N-butyl ether, propylene glycol, and DOSS. None of the samples were found to be in excess of EPA's benchmark levels for protecting aquatic life (EPA, 2010). DOSS raised much concern by many during the DWH response due to its low volatility and bioactivity (Lubchenco et al., 2012). A new analytically method was introduced during the oil spill to quantify the presence of DOSS in seafood (Rick A. Flurer et al., 2010, Samuel Gratz et al., 2010). After repeated laboratory tests, results indicated that DOSS concentration in the seafood were at least three orders of magnitude below the levels of concern (Gohlke et al., 2011, Hayworth and Clement, 2012).

The debate about the advantages and disadvantages of using dispersants for managing marine oil spills has been ongoing for some time (Lee et al., 1985, Lönning and Hagström, 1976, Mitchell and Holdway, 2000, Singer et al., 1996). It is necessary for oil spill response decision-makers to have a comprehensive understanding regarding the toxicity of dispersants to humans and the environment to fully understand the ramification of this debate. Most toxicity studies related to Corexit were done on fish, fish larvae, and marine microbial species (Fuller et al., 2004, George-Ares and Clark, 2000, Singer et al., 1993, Wardrop et al., 1987). Very few in vitro data are available to quantify the toxicity of Corexit using individual mammalian cells. It would be of great significance to understand the toxicity of Corexit on individual mammalian cells because we can learn which part of the human body is more vulnerable to Corexit, and these in vitro data can predict adverse effects of Corexit in vivo (McKim, 2010).

1.3 Toxicity studies

A limited number of studies have been done to quantify the toxicity of Corexit. Judson et al. (2010) investigated the in vitro cytotoxiciy by using HepG2 cell on eight commercial dispersants: Corexit 9500, JD 2000, DISPERSIT SPC 1000, Sea Brat #4, Nokomis 3-AA, Nokomis 3-F4, ZI-400, and SAF-RON GOLD. Result showed that the LC50 of DISPERSIT SPS 1000 is 28 ppm; Corexit 9500 is 120 ppm; Nokomis 3-F4 is 180 ppm; Nokomis 3-AA is 200 ppm; Sea Brat #4 is 410 ppm; ZI-400 is 420 ppm; JD 2000 and SAF-RON GOLD are more than 1000 ppm. These researchers also carried out high-throughput assays to investigate whether these dispersants can cause endocrine disruption. Their results showed that Corexit did not cause endocrine disruption.

Bandele et al. (2012) used HepG2/C3 to assess the in vitro toxicity of Corexit 9500, Corexit 9527, ZI 400 and DOSS by measuring the number of double strand DNAs as a proxy for living cells. Corexit 9500 and Corexit 9527 showed a similar dose-dependent cytotoxicity from 0 ppm to 400 ppm, while ZI 400 showed less toxicity. The LC50 of both Corexit 9500 and Corexit 9527 was around 240 ppm. Two time points (24 hours and 72 hours) were used in this study and the results show these two time points exhibited similar LC50 levels.

HepG2 cell was used by Judson et al. (2010) and Bandele et al. (2012) to find the in vitro toxicity of Corexit 9500. Two different results were found: Judson et al. (2010) showed the LC50 of Corexit 9500 was 120 ppm while Bandele et al. (2012) showed the LC50 of Corexit 9500 was 240 ppm. This variance between toxicity endpoints is due to differences in experimental methods. Judson et al. (2010) measured the mitochondria activity to interpret the amount of living cells, while Bandele et al. (2012) quantified the double strand DNA to interpret cells viability levels.

The generation of reactive oxygen species (ROS) is another indicator of cell dysfunction. Bandele et al. (2012) showed that within 24 hours, ROS level in cells exposed to Corexit 9500 increased 4.5 fold, and within 72 hours ROS levels increased by 7 fold. DOSS increased ROS levels by 5 fold within 24 hours and by 9 fold within 72 hours. These results suggest that DOSS contributed the ROS generation in the cells exposed to Corexit 9500.

George-Ares and Clark (2000) collected acute in vivo toxicity data of Corexit 9527 to10 marine species and of Corexit 9500 to 27 marine species. Their results demonstrated that Corexit 9527 and Corexit 9500 had low (LC50>100 ppm) to moderate (LC50 > 1 to 100 ppm) toxicity to most marine species in laboratory testing. The toxicity of marine species was highly variable; for example, the 48 to 96 hours toxicity of fish to Corexit 9500 ranged from 140 ppm to 96,500 ppm and the 48 to 96 hours toxicity of crustaceans ranged from 1.6 to 2500 ppm. George-Ares and Clark (2000) also suggested that a 4 hour time point should be a better indicator of the actual condition because the dispersant diluted quickly after application.

During the DWH oil spill, 48,000 workers were involved in the cleanup efforts. About 2914 m3 dispersant out of the 7000 m3 dispersant used were applied from aircraft (the rest was applied near the well head); workers on site could have inhaled some of the dispersant mist and their skin could have been affected by the dispersant. Therefore, the National Institute for Occupational Safety and Health (NIOSH) conducted research mainly focusing on the acute pulmonary, brain, and skin response exposure to dispersant (Castranova, 2011). These results are summarized below.

In an effort to understand the pulmonary effects of dispersant, male rats were exposed to Corexit (27mg/m3) for 5 hours. Pulmonary effects of Corexit after inhalation on the first day and seventh day were examined with lactate dehydrogenase (LDH), and albumin as an indicator

of lung injury and macrophages. Neutrophils, lymphocytes, eosinophil were quantified to evaluate the inflammation. No significant results were found in any of these assays. The study suggested the inhalation of Corexit did not initiate lung inflammation (Roberts et al., 2011).

The inhaled Corexit might permeate the brain through the olfactory system and influence the central nervous system (CNS) function. Sriram et al. (2011) studied the potential neurological risk of Corexit by exposing the male rats with Corexit (27mg/m3) for five hours, the effect of Corexit on brain was evaluated in discrete brain areas at the first day and seventh day. Result showed partial loss of olfactory marker proteins in the brain, decreased tyrosine hydroxylase protein in the striatum, and increased expression of glial fibrillary acidic protein in the hippocampus and frontal cortex. This evidence suggests imbalances in neurotransmitter signaling after acute exposure to Corexit.

Anderson et al. (2011) studied the immnuotoxicological effect of Corexit and DOSS on the workers involved in the cleanup efforts of the DWH oil spill reported to have pulmonary and dermatological problems. Results of the study showed both Corexit 9500 and DOSS-induced dermal irritation and lymphocyte proliferation in a dose-dependent manner. EC3 value, a parameter to evaluate the skin sensitizing potency of contact allergens, classifies Corexit as a potent sensitizer and DOSS as a moderate sensitizer.

The combined effect of Corexit and oil raised concerns because studies have shown that Corexit-oil mixtures may be more toxic than Corexit or oil alone (Hemmer, 2011, Rico-Martínez et al., 2013). In 2013, the marine rotifer Brachionus plicatillis was used to test the toxicity of oil, Corexit 9500, and an oil-Corexit 9500 combination. The result demonstrated the toxicity of Corexit 9500 was similar that of oil, but the combination had much higher toxicity of up to 52 fold increase(Rico-Martínez et al., 2013). Hemmer (2011) used two marine organisms, the mysid

shrimp (Americamysis bahia) and the inland silversides (Menidia beryllina) from the Gulf of Mexico to test the in vivo toxicity of eight commercial dispersants. Result suggested all eight dispersants were less toxic than the oil-dispersant mixture.

The in vitro toxicity of water accommodated fraction (WAF), a mixture of oil, dispersant and sea water, on A549 cell line was studies by Wang et al. (2012). Results suggested dose-dependent effects of WAF on A549 cell line both at 2 hour and 24 hours time scales, and the toxicity from these two time points showed similar LC50. The WAF in this study was prepared using Corexit 9500 and Corexit 9527 among others. Result shown the toxicity of dispersed Corexit 9500 and dispersed Corexit 9527 were similar. In an effort to understand the mechanism, lactate dehydrogenase assay, morphology observation, and quantification of protein Caspase-9 were done to measure necrosis and apoptosis. Results showed both necrosis and apoptosis were involved in the toxicity mechanism (Wang et al., 2012).

Studies have shown dispersed WAF exerts a higher bioactivity. Milinkovitch et al. (2012) exposed juveniles of Liza aurata to dispersed and non-dispersed oil. Results suggest PAHs were accumulated in the biliary metabolites when marine organisms were exposed to the dispersed oil. Also, Major et al. (2012) found increased complexity of dispersant-oil WAF when compared with the oil WAF. Increased complexity refers to high molecular weight compounds such as alkyl derivatives, esters and PAHs. Although the complexity was increased, the in vitro toxicity of the WAF did not increase.

1.4 Literature review on different cell lines used for Corexit toxicity

When compared to in vivo toxicity data, the in vitro toxicity data can be produced in a comparatively short time period, at a lower price, with less viability (Cohrssen et al., 1989). It

can also serve as an alternative to in vivo method for predicting the toxicity of a substance (Ekwall et al., 1990). Typically, toxicity studies of oil and dispersant in vivo usually expose marine species with the dispersant or dispersed oil for some time. Results may vary due to the differences between species, sex and the life stage of the species (George-Ares and Clark, 2000), while in vitro cell culture promise a more consistent result (Ekwall et al., 1990).

Brain matter consists of neuronal and glial cells. Neurons are electrically excitable cells that processes and transmits information using electrical and chemical signals (Myers, 2013). Glial cells represent one of the most common neuron tissue cells; they support neural growth and metabolism (Stacey and Viviani, 2001). The interaction between glia and neurons in brain matter resist the toxic insults of unknown substance (Stacey and Viviani, 2001). The *in vitro* method is preferable to *in vivo* method because it can help interpreting the result in a more explicit way and also provide the mechanism of toxicity. In our study, a neuronal cell (H19) and a glial cell (1321N1) were selected to test the toxicity of Corexit. H19-7 cell line has been used to test the toxicity of alpha-synuclein, a amyloid protein precursor (Sung et al., 2001); pyrrolidine derivative of dithiocarbamate, a cell death inducer (Min et al., 2003). Furthermore this cell line was also used to determine neuroprotective effect of 17β-estradiol, genistein, and daidzein, and phytoestrogens, which are believed to reduce the risk of Alzheimer disease (Pan et al., 2012). 1321N1 has been used to test the toxicity of cadmium (Cd) (Lawal and Ellis, 2011); scorpion venom (Mulligan et al., 2003); and brefelamide, an aromatic amide which can inhibit the growth rate of 1321N1 human astrocytoma cells (Honma et al., 2009).

The other cells used in this study are derived from kidneys. The human embryonic kidney cell line HEK 293, and HK-2, an immortalized proximal tubule epithelial cell line. HEK 293 is a well-established renal cell line to test toxicity effects. It has been used to test the

toxicity of wall carbon nanotubes (Cui et al., 2005), chitosan-DNA nanoparticles (Cui et al., 2005), arsenite (Kirkpatrick et al., 2003), and flavonoids (Lee et al., 2009). HK-2 has been used to test the renal protective effect of emodin, a component in Chinese herb (Wang et al., 2007); and the toxicity effect of inorganic arsenic (Peraza et al., 2003), triptolide (Shu et al., 2009), and oxalate (Jeong et al., 2005).

B16/BL6 is a mouse melanoma cell line which has been used to test the toxicity of trivial metals like La^{3+}, Ce^{3+}, Nd^{3+}, Gd^{3+}, Yb^{3+}, Al^{3+} (Sato et al., 1998), polyamines and novel polyamine conjugates (QARAWI et al., 1997), antitumor drugs (Woiniak et al., 2005), and San-bai-tang (SBT), a Chinese herbal formula (Ye et al., 2010).

Following the exposure of cells to toxicants, morphological changes in the cell shape, like blebbing and vacuolization can be observed by using light microscopy (Ekwall, 1983). The alternation of cell growth rate is another index of cell toxicity. The replication rate of cells can be measure by cell count, DNA content, biological end point, and protein content, or enzyme activity (Costa, 1979). The MTT assay used in our study falls into the third category, by measuring the absorbance of biochemical dyes which can be taken up by living lines and the absorbance compared with the control to provide the viability index (Kruse, 1973). Other commonly used endpoint assay to monitor toxicity effects include the neutral red assay which measures the vital dye uptake, and the lactate dehydrogenase leakage assay which measures the release of cytoplasmic activity (Stacey and Viviani, 2001). Measuring the biochemical and metabolic alternations (e.g. using HPLC to measure the DNA, RNA precursor, which is believed to be the indication of toxicity) is another common approach (Bianchi, 1982).

MTT (3-(4,5-Dimethylthiazol-2-yl)-2,5-diphenyltetrazolium bromide) assay was used in this effort to investigate the viability of cells on the basis that the yellow tetrazolium salts can be

converted to dark blue formazan in the mitochondria of living cell lines (Twentyman and Luscombe, 1987). However, studies have shown the serum concentration, serum type, medium type, and the lipophilicity of the substances can impact the results of MTT assays (Ekwall et al., 1990).

According to research done by Zhang and Cox (1996), when the serum concentration was less than 5%, the result of MTT assay will be minimally affected. However, if the concentration of serum is larger than 10%, the result of MTT assay would be increased by 20%. When the concentration of serum is between 5% and 10%, no change can be observed in total mitochondria activity. It was shown in another study that the serum itself will cause false positive results when the concentration ranges from 1% to 10% (Funk et al., 2007).

The result of MTT assay can also be impacted by the serum type. Gülden et al. (2006) showed an additional 18% supplement of hours serum (HS) in the media which contain 2% fetal bovine serum (FBS) can increase LC50 value by 4.2 to 50 fold, while an additional 18% FBS can lead to a 1.5 to 10.4 fold increase in LC50. This is because serum contains protein and lipids that can bind to the potential toxins used in the MTT assay, therefore decrease the bioavailability of the target toxins (Gulden and Seibert, 2003, Seibert et al., 1989). The lipophilicity of a potent toxin is another factor that will influence the result of cytotoxicity assays. Researchers have shown that the cytotoxicity potency of chemicals in general is positively correlated with the lipophilicity (Ahlers et al., 1991).

Gülden and Seibert (2005) have shown that there is an increased correspondence between acute *in vivo* toxicity and *in vitro* toxicity date when using serum-free media. So in an effort to allow a better understanding of a potent toxin, a selective media, which is serum-free supplemented with basic nutrients and growth factors, is recommended (Barnes and Sato, 1980)

in toxicity studies. Serum-free media can eliminate the over growth of fibroblasts as these cell lines tend to grow faster in serum supplemented media (Ekwall et al., 1990). Also, the use of serum-free media *in vitro* can have a better prediction of *in vivo* data when the study objective is interactions between cell and hormones or drugs (Ekwall et al., 1990). Certain types of cell can grow in a more efficient and differentiated way in serum-free media, the HEL222 human lung epidermoid carcinoma cells (Bourdeau, 1990) .

1.5 Potential problems with *in vitro* studies

It is difficult to interpret the actual exposure concentration of oil, dispersant because WAF contain a mixture of compounds with various volatility, lipophilicity and solubility (Coelho et al., 2013). Coelho et al. (2013) also pointed out that Rico-Martínez et al. (2013) study did not characterize the actual exposure concentration to allow comparison with previous results. The second common problem is the compound used in study to quantify the results. Most studies reported their result by the % of WAF or the % of chemically enhanced water accommodated fraction (CEWAF). However, according to a NRC (2005) report, the LC50 should be reported in total petroleum hydrocarbons (TPH), because other studies have found a stronger relationship between TPH and oil toxicity (Clark, 2001).

The third problem is variations in WAF preparation methods used by different labs. When preparing WAF, the order of putting oil and dispersant, the mixture time, the salinity, pH, and degree of the artificial sea water, and many other factors can influence the actual amount of oil being dispersed under laboratory condition (NRC, 1989). The interpretation of toxicity data differs greatly depending whetherWAF or CEWAF is used, because different preparation methods can result in different amount of oil being distributed in the water phase. A standard

method needs to be established to solve this problem, Singer et al. (2000) published a method to prepare the WAF. However, the validity of the proposed method has been questioned by others (Barron and Ka'aihue, 2003).

The forth problem is the uncertainty in oil-dispersant ratios. In the Rico-Martínez et al. (2013) study, the application ratio of oil to dispersant was calculated by comparing the amount of spilled oil (780,000 m^3) to dispersant (7,000 m^3) (Kujawinski et al., 2011). However, this comparison overlooked the fact that some of the oil was burned, skimmed, evaporated, dissolved, and naturally dispersed (the exact fate of oil is shown in Figure1-3). It was later modified so that the actually ratio of dispersed oil is 16% (Lubchenco et al., 2012), which means approximately 124,800 m^3 oil was dispersed by 7000 m^3 dispersant, so the real ratio of oil to dispersant was approximately 1:20. However, the oil : dispersant ratio in previous studies varied (1:20, 1:40, 1:80, 1:130), thus it is difficult to compare these results (Coelho et al., 2013).

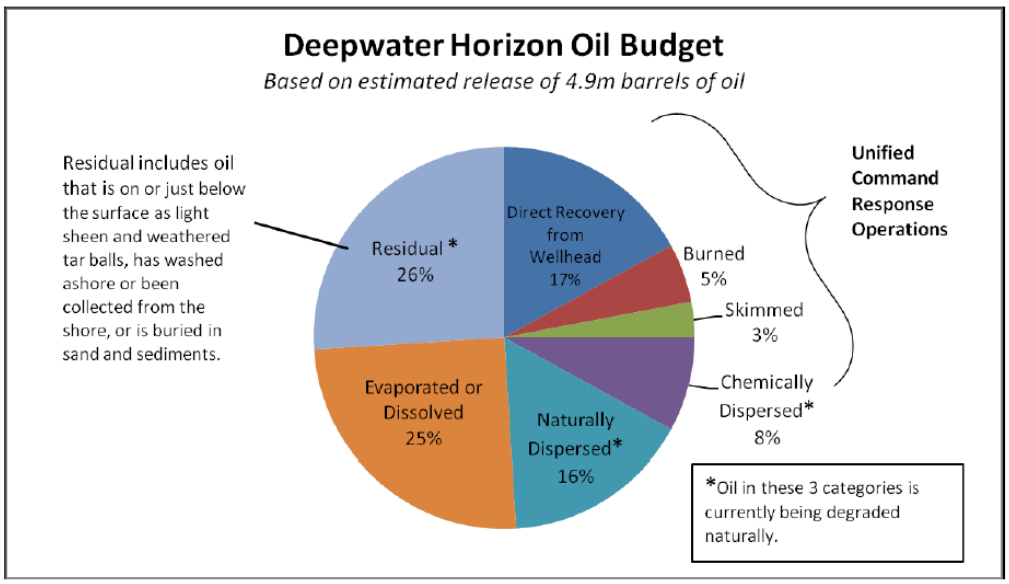

Figure 1-3 Deepwater Horizon Oil Fate (UCBerkeley, 2010)

1.6 Research objectives of this study

The objective of this study is to investigate the *in vitro* toxic effects of Corexit on various cell lines. We hypothesize that exposure to Corexit would decrease the cell viability by causing mitochondria dysfunction, apoptosis and oxidative stress. In this study, different doses of Corexit was incubated with human and animal cell lines obtained from various tissues (neuronal, glial, kidney, skin). The effects are assessed using the 3-(4,5-Dimethylthiazol-2-yl)-2,5-diphenyltetrazolium bromide (MTT) assay, and the cell viability was quantified by the colorimetric method.

CHAPTER 2. Toxicity studies

2.1 Material and Methods

2.1.1 Chemicals and reagents

Thiazolyl Blue Tetrazolium Bromide (MTT), Trypsin-EDTA solution, and dimethyl sulfoxide (DMSO) were purchased from Sigma/Aldrich (St. Louis, MO).

2.1.2 Cell culture

Cells derived from lung, liver, heart, muscle, brain and reticuloendothelial systems have been widely used to conduct toxicity tests (Ekwall et al., 1990). Among these cell types, the human fibroblast cell and tumor cell line were widely used because they can be more easily cultured (Ekwall et al., 1990). Five types of cell lines were selected in our study. A skin tumor cell line (B16/BL6); a neuronal cell line (H19-7); a glial cell line (1321N1); and two kidney cell lines (HEK 293 and HK-2).

Skin Tumor Cells (B16/BL6)

B16/BL6 cells were grown in BL6/C57 mice by injecting B16 melanoma cells into the derma of both ears to create a primary tumor. B16/BL6 cells were cultured in DMEM supplemented with 10% FBS (10% final concentration). Cells were propagated in 75 cm^2 tissue culture flasks (Figure 2-1), harvested by trypsinization after reaching 80% confluence for 3 to 4 days, and then plated into 96 well plate (Figure 2-2) at a density of 1 x 10^4 to 5 x 10^4 cells/ml media by using a multi-channel pipette (Figure 2-3). Cells were incubated in an incubator at 37

˚C and with the supplement of 5 % CO_2. The cultures were used within 20 passages after the cells were received.

Figure 2-1 Cell culture method employeed in this study

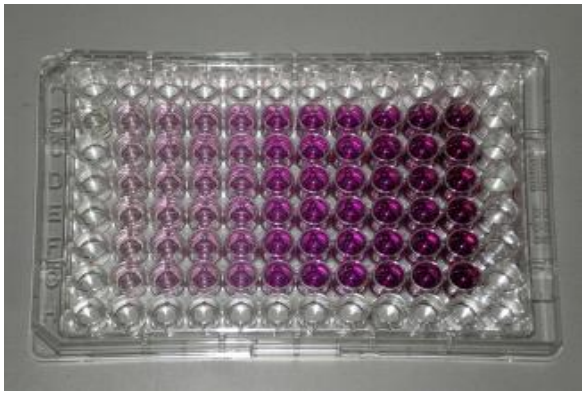

Figure 2-2 96 well plate used in this study (96 wells per plate)

Figure 2-3 Multi-channel pipettes used in this study

Neuronal Cells (H19-7)

H19-7 cell line is a neuronal cell. The H19-7 cells, originally derived from hippocampi dissected from embryonic day 17 (E17) (Morrione et al., 2000). H19-7 cells were maintained in Dulbecco's modified Eagle's medium with 4 mM L-glutamine adjusted to contain 1.5 g/L sodium bicarbonate and 4.5 g/L glucose supplemented with 10% fetal bovine serum, 200 μg/ml G418, and 1μg/ml puromycin in flasks coated with 15 μg/ml poly-L-lysine. Cells were propagated in 75 cm^2 poly-L-lysine coated tissue culture flasks, harvested by trypsinization after reaching 80% confluence for 3 to 4 days, and then plated into poly-L-lysine coated 96 well plates at a density of 2 $\times 10^5$ cells/ml. They were equilibrated in a humidified atmosphere of 5% CO_2/95% O_2 at an air temperature of 34˚C. The cultures were used within 20 passages after the cells were received.

Glial Cells (1321 N1)

1321 N1 is derived from glial cell in human brain. 1321N1 is a human astrocytoma cell line isolated in 1972 as a sub clone of the cell line 1181N1 which in turn was isolated from the parent line U-118 MG, one of a number of cell lines derived from malignant gliomas by J Ponten. 1321N1 are neuronal derived inflammatory cell line that was cultured in DMEM supplemented with 10% FBS. Cells were propagated in 75 cm^2 tissue culture flasks, harvested by trypsinization after reaching 80% confluence for 3 to 4 days, and then plated into 96 well plates at a density of 2 x 10^4 to 4 x 10^4 cells per 10 ml. Cells were incubated at 37˚C and 5 % CO_2. The cultures were used within 20 passages after the cells were received.

Kidney Cell-I (HEK 293)

Human embryonic kidney 293 (HEK293) cells were isolated from primary human embryo kidney cells and transformed by sheared adenovirus 5 DNA (Shaw et al., 2002). HEK293 was cultured in DMEM supplemented with 10% FBS (10%) final concentration. Cells were propagated in 75 cm^2 tissue culture flasks till it reaches 90% confluence. For splitting the cells, we harvested the cells with 1 ml trypsin for 5 minutes, then mixed the trypsinzed cells with 9 ml media, plated these cells into 96 well plates by using 100µl pipettes at a density of 2×10^5 cells/ml. Cells were incubated at 37 ˚C and 5 % CO2.

Kidney Cell-II (HK2)

HK-2 (human kidney 2) is a proximal tubular cell (PTC) line derived from a normal kidney. Advantage of HK-2 cells is that they can reproduce experimental results obtained with freshly isolated PTCs. HK-2 cells were cultured in keratinocyte serum-free medium (K-SFM) supplemented with 0.05 mg/ml BPE and 5 ng/ml EGF and 5% Fetal Bovine Serum (FBS). Cells were propagated in 75 cm^2 tissue culture flasks, harvested by trypsinization after reaching 80% confluence (3-4 days), and then plated into 96 well plates at a density of 2×10^5 cells/ml. Cells were incubated at 37˚C and 5 % CO_2. The cultures were used within 20 passages after the cells were received.

2.1.3 Treatments

Prior to each experiment, Corexit was diluted to 1000 ppm in double distilled water (ddH_2O) and subsequently diluted to 20 to 200 ppm using the cell culture media. Five different concentrations of Corexit (20, 40, 80, 160, and 200 ppm) were used to assess cytotoxicity in each cell line. Corexit was exposed to cell lines for a time period of 48 hours. The 48-hour time

represents a relatively long exposure period for *in vivo* tissue based toxicity. After incubation, cell viability was measured with the MTT assay under two different metabolic conditions: one with serum, which represents a well-nourished state; and the other without serum, which represents a nutritionally-compromised state. Rational for using these two states is to study the toxicity of Corexit at both nourished and undernourished systems. Each concentration of test agent was tested in duplicates per set of the 96-well system used in this study with every assay performed three times.

2.1.4 Cytotoxicity Assays

MTT assays were performed using B16/BL6, H19-7, 1321N1, HK2, HEK293 cells as an indicator of cytotoxicity. The principle of this assay is the mitochondrial reductive conversion of the yellow colored MTT, a yellow tetrazole reagent to a blue formazan by alive mitochondria of viable cells (Berridge et al., 1995, Mosmann, 1983). The chemical structure of MTT and its reduced form were shown in Figure 2-4. The MTT assay was performed following procedures in Dhanasekaran et al. (2006)'s study. Briefly, after incubation of Corexit with serum-fed and serum-free media for 48 hours, MTT was added at a final concentration of 1 mg/ml. The medium was discarded after the incubation for 4 hours at 37 °C and the insoluble dark blue formazan crystals were dissolved in 100 µl of DMSO. Absorbance was subsequently measured at 570 nm with a reference wavelength of 630 nm using a microtiter plate reader (Synergy HT, Bio-Tek Instruments Inc., Winooski, VT, USA) shown in Figure 2-5.

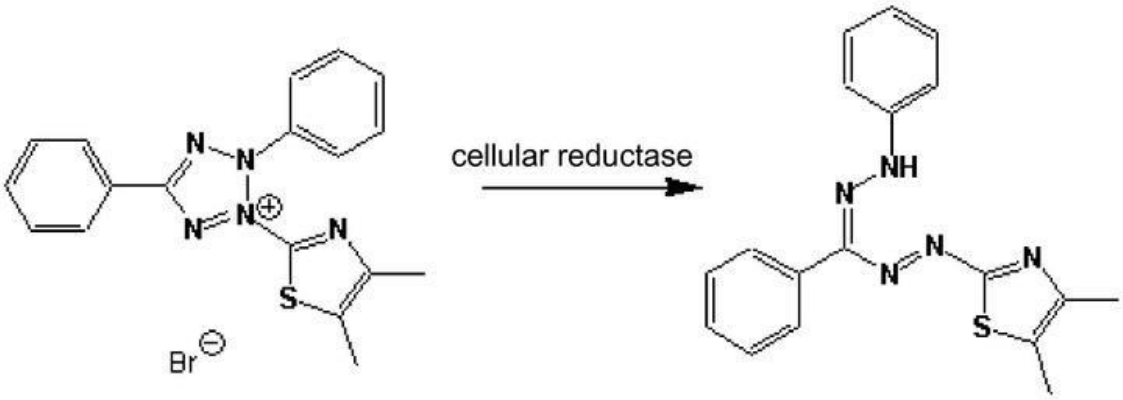

Figure 2-4 Chemical composition of MTT and its reduced form

Figure 2-5 Microplate reader (Synergy HT, Bio-Tek Instruments Inc., Winooski, VT, USA)

2.1.5 Statistical analysis

Values are expressed as means ± standard error of the mean (SEM) for each type of cell line. Statistical analyses were performed using two sample t-test. $P < 0.05$ was considered to indicate statistical significance (Wan et al., 1999). All results summarized in this thesis were obtained from three independent experiments (duplicates for each experiment).

2.1.6 Estimation of LC50

The viability of the cells were obtained by dividing the reading of cells treated with Corexit (0, 20, 40, 80, 160, 200 ppm) by the reading of cells treated with non-toxic dosage of Corexit (0 ppm) and multiplying the value by 100. The reading refers to the absorbance we obtained from the microplate reader (Synergy HT, Bio-Tek Instruments Inc., Winooski, VT, USA). A set of example raw data are shown in Table 2-1 to illustrate the procedure used for calculating cell viability. A dose-dependent curve can be generated by Prism, a commonly used software to calculate LC50. By using the log concentration of Corexit as X axle, cell viability as Y axle. A regression curve was generated according to the formula Y=100/(1+10^((X-LogLC50)) by the software for a better indication of the overall trend of the induced cell viability. The regression curve was shown in Table 2-1.

Table 2-1 Example raw data of Corexit induced cytotoxicity on human kidney cell-II (HK-2).

HK-2 cell incubated under serum-free condition				
Corexit (ppm)	Average (n=6) Absorbance	Viability (%)	Std.Dev (%)	SEM (%)
0	0.456875	100		
20	0.439125	96	4	1.44
40	0.412375	90	6	2.16
80	0.315	69	5	1.93
160	0.072625	16	1	0.41
200	0.07275	16	1	0.47

Average refers to absorbance at 570 nm with a reference wavelength of 630 nm using the 96 well plates (Synergy HT, Bio-Tek Instruments Inc., Winooski, VT, USA). Cells treated with 0 ppm Corexit was considered as 100% viability. Divide the reading of a treated dosage (20, 40,

80, 160, 200 ppm) by the reading of non-treated dosage then multiply by 100 to get the percentage viability.

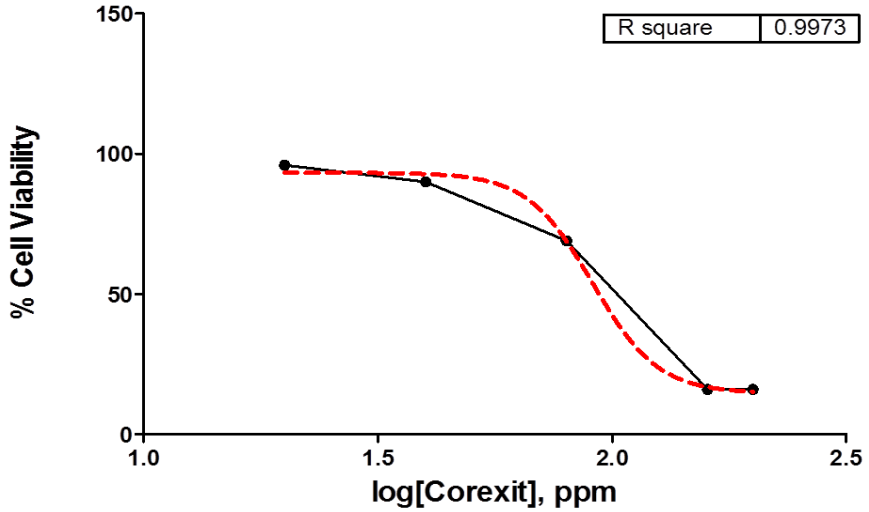

Figure 2-6 Changes in cell viability at various Corexit concentrations.

The log concentration of Corexit is X axis, and the cell viability is in Y axlis. By fittting the curve, the 50% of the cell death was established by using prism software.

2.2 Results

2.2.1 Effect of Corexit on skin tumor cells

In cell-based toxicological studies, cancer cell lines are the first preference for testing the toxic potential of any new chemical compound. Reason for this is that cancer cells are highly-specialized cells that have been transformed to a much simpler, more primitive stage and thus posses the ability to grow continuously by division (Ekwall et al., 1990). Secondly, due to the high cell division rate, they are more vulnerable than most normal cells to any toxin. Hence, they provide a sensitive cellular model for toxicological investigations that can be done rapidly and accurately.

For establishing the toxicity of Corexit, in the current study different concentrations of Corexit (20, 40, 80, 160, and 200 ppm) were incubated with B16/BL6 cell line for 48 hours under two different metabolic conditions. The data show Corexit exhibits a dose dependent toxicity in the skin tumor cell line, as illustrated in Figure 2-8 ($n=6$, $p<0.005$). The toxicity in serum-fed condition was not as high as in the serum-free condition. Almost 100% of cell death was observed under serum-free conditions, while the same dose exhibited 40% cell death under serum-fed condition. The LC50 value for B16/BL6 cells, under serum-free state, was found to be 16 ppm. We did not find 50% or more cell death in serum-fed vials, which limited our ability to calculate LC50 for Corexit under this condition.

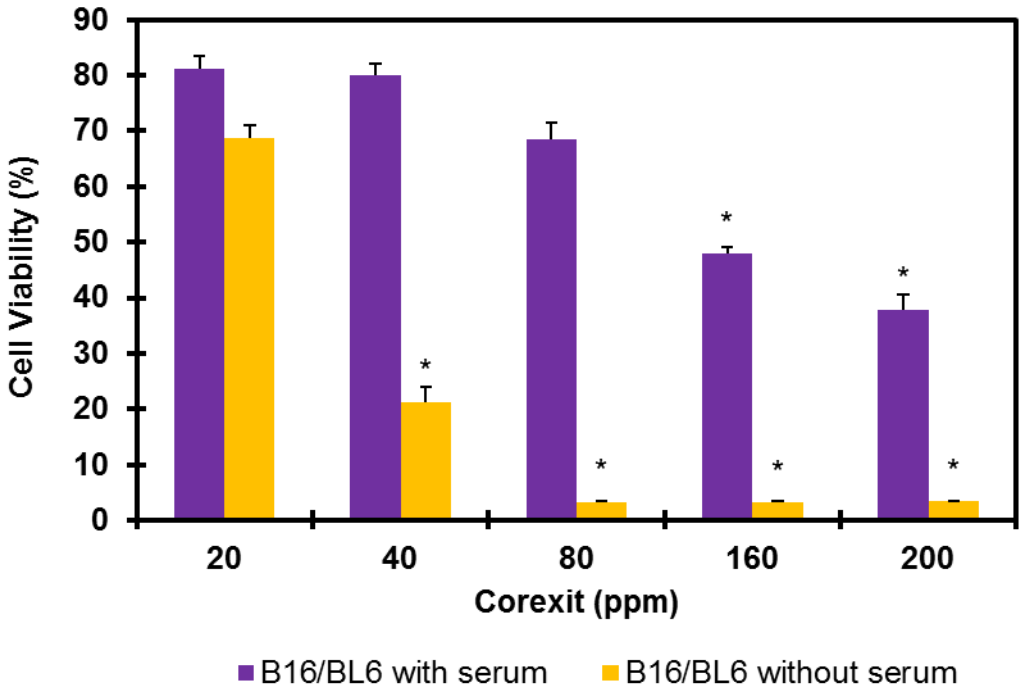

Figure 2-8 Effect of Corexit on skin tumor cells

Cells were treated with different concentration of Corexit for 48 hours. At the end of incubation period, the MTT assay was performed to assess the cell viability as described before.

The percentage of cell viability was calculated by dividing the reading of the target well to the control. Control cells were incubated in Corexit free media run in parallel to treatment groups. The data are expressed as mean ± of three independent experiments (duplicates in each experiment). (*) indicates a statistically significant difference compared to controls ($p<0.005$).

2.2.2 Effects of Corexit on neuronal cells

Rat hippocampal neuronal cultures are well-established cellular model where pre- and post-synaptic neuronal interaction can be studied. Another reason for selecting this neuronal cell line is that the biological implications of the hippocampus, an area of the brain that is considered to play a central role in controlling learning and memory formation. It is strongly believed that the chronic neurotoxicity affects the attentive and mnemonic functions in the long run and eventually they would deteriorate the quality of life. Hence, by studying the impact of Corexit on hippocampal neurons we expected to quantify Corexit toxicity effects, though indirectly, on learning and memory functions of mammalian systems.

To evaluate cytotoxic effects on mammalian hippocampal neuronal cells following Corexit treatment, undifferentiated H19-7 hippocampal neurons were incubated with Corexit (20, 40, 80, 160, and 200 ppm) for 48 hours. We found Corexit significantly reduced cell viability dose dependently under both serum-free and serum-fed media conditions (Figure 2-9, $n=6$; $p<0.005$). However, the toxicity of Corexit was more prominent in serum-free state with a reduction in cell viability by 80% in comparison to 20% reduction observed in serum-fed neuronal cells (Figure 2-9). Additionally, in serum-free media a more conspicuous dose-dependent effect of Corexit was observed in terms of neuronal cell death. Serum-free media represents an unnourished state that compromises the defense mechanisms of a cell and the respective tissue and organ. Thus, in an already compromised mammalian system the toxicity of

Corexit to CNS would increase by many folds. The LC50 for H19-7 cell was 70 ppm. Similar to the cancer cell line data set, we were unable to deduce LC50 values for the H19-7 cells under serum fed conditions.

Figure 2-10 shows the general morphology of control cells and Corexit exposed cells. Figure 2-10A shows the morphology of the control cell after 48 hours in serum-free media. Figure 2-10B, 2-10C and 2-10D shows the morphology changes of Corexit 80, 160 and 200 ppm after 48 hours incubation in serum-free media. With increasing doses of Corexit, cells started to shrink and decrease in number. Figure 2-10A shows Control group where the cells were incubated under normal conditions. Figures 2-10B (80 ppm), C (160 ppm) and D (200 ppm) represents the increasing concentration of Corexit and the correspondingly decreasing amount of living cells.

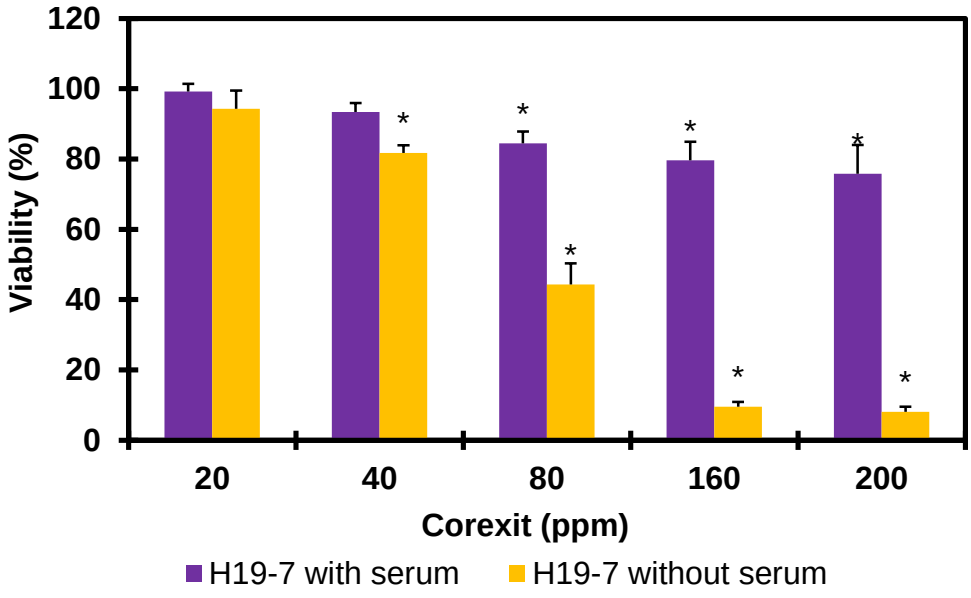

Figure 2-9 Effect of Corexit on neuronal cells.

Cells were treated with different concentration of Corexit for 48 hours. At the end of incubation period, the MTT assay was performed to assess the cell viability. The percentage of cell viability was calculated by dividing the reading of the target well to the control. Control cells were incubated in Corexit free media run in parallel to treatment groups. The data are expressed as mean ± of three independent experiments (duplicates in each experiment). (*) indicates a statistically significant difference compared to controls ($p<0.005$).

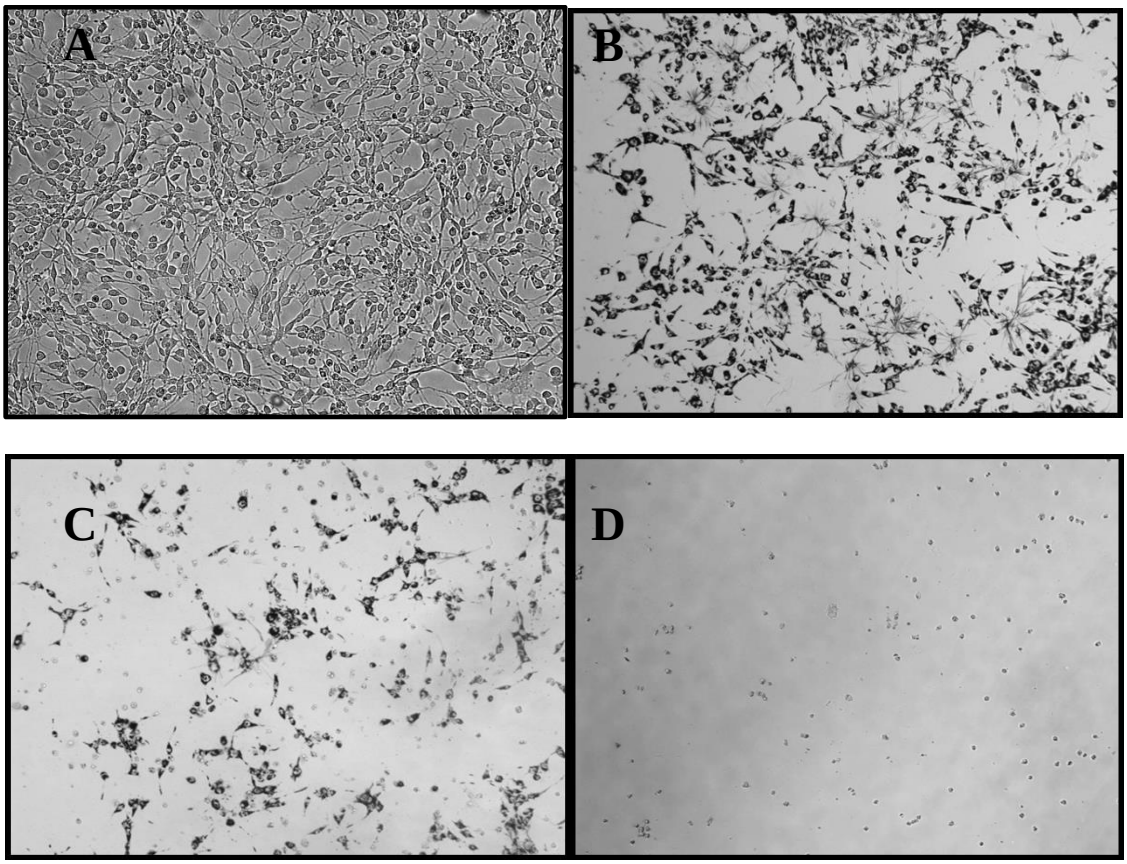

Figure 2-10 Morphological characterizations of neuron cell.

Cells were treated with different concentrations of Corexit for 48 hours at 37 ˚C in an incubator with 5% CO_2. At the end of 48 hours of exposure cells were washed with PBS and

visualized under microscope (magnification 10X). (A) Control; (B) 80 ppm of Corexit; (C) 160 ppm of Corexit; (D) 200 ppm of Corexit.

2.2.3 Effects of Corexit on glial cells

The human astrocytoma cells (glial cell line) used in these studies were originally isolated from primary cultures of cerebral glioblastoma multiforme (PontÉN and Macintyre, 1968). These are neoplastic cells (tumor cells) from a specific type of neoplasm of the brain. They originate in a particular kind of glial-cells, star-shaped brain cells in the cerebrum called astrocytes. Being a cancer cell line of neuronal inflammatory cells, 1321N1 cells proved to be a valuable toxicological *in-vitro* model for studying the toxic effects of Corexit.

Similar to other cell lines, Corexit was incubated, as mentioned before, in different concentrations with this cell line. Results demonstrate the expected trend of cellular toxicity as exhibited by rat hippocampal H19-7 cell lines, in both serum-fed and serum-free states (Figure 2-9, $n=6$; $p<0.005$). However, these cells were found to be more vulnerable to Corexit and induced cell death at much lower concentrations ranging from 20 ppm to 40 ppm. The higher level of toxicity could be attributed to their neoplastic nature. For 1321 N1 cell, the LC50 was 33 ppm (Figure 2-11). Serum-free conditions exacerbated the toxicity effects. Corexit toxicity increased many-folds under serum-free conditions resulting in almost 100% cell death even at 40 ppm (Figure 2-11). Indirectly, Corexit toxicity to the astroglial cells, being inflammatory cells of CNS that play a vital role in protecting neuronal cells, suggesting that by affecting both astroglial and neuronal cells Corexit could potentially pose some threat to CNS.

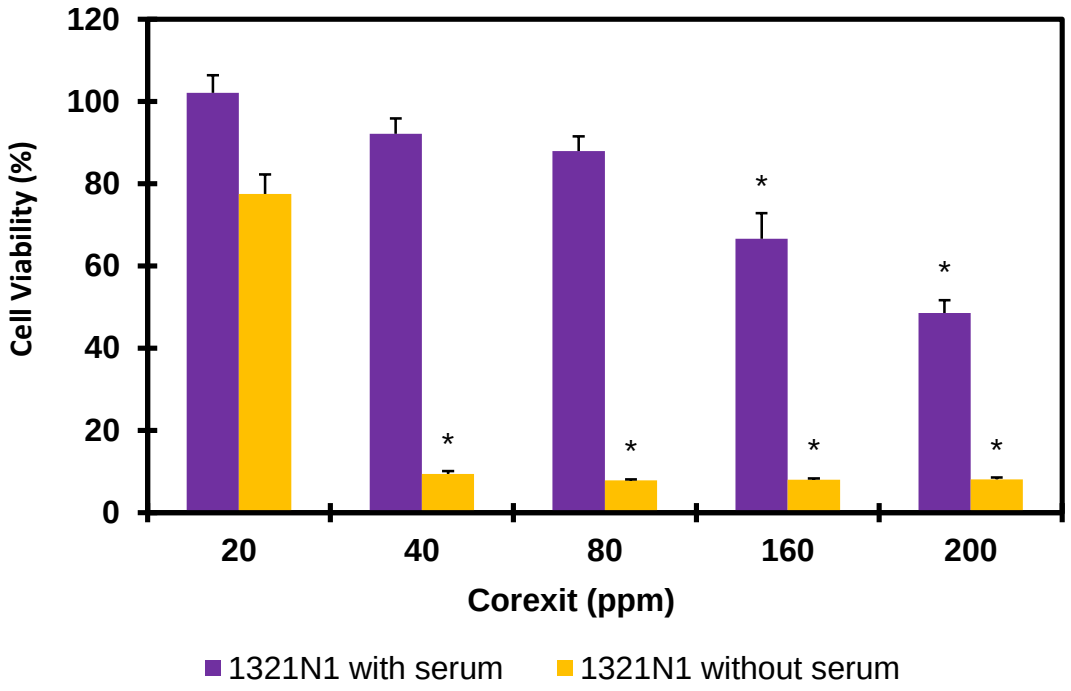

Figure 2-11 Effects of Corexit on glial cells.

Cells were treated with different concentration of Corexit for 48 hours. At the end of incubation period, the MTT assay was performed to assess the cell viability as described in the Chapter 2. The percentage of cell viability was calculated by dividing the reading of the target well to the control. Control cells were incubated in Corexit free media run in parallel to treatment groups. The data are expressed as mean ± of three independent experiments (duplicates in each experiment). (*) indicates a statistically significant difference compared to controls ($p<0.005$).

2.2.4 Effects of Corexit on kidney cells

Liver and kidney are the two key organs that remove toxin substances from a mammalian body; therefore, they are one of the best candidates for toxicity testing. Toxic byproducts of cellular metabolism, foreign particles and transformed metabolites of xenobiotics are efficiently removed by kidneys. Hence, it is of great significance to study the impact of Corexit on kidney cells. To do so, we selected two well-established and extensively used human kidney cell lines i.e. HK-2 cell line (Gunness et al., 2010) and HEK293 cell line. Studies showed HEK293 cell line is a valid model to indicate the nephrotoxicity of a toxin to human beings. HK-2 is an immortalized proximal tubule epithelial cell line from a normal adult human kidney. It retains the phenotypic characteristics of a well grown differentiated kidney cell. In addition, HK-2 cells possess functional characteristics of proximal tubular epithelium (Na+ dependent/phlorizin sensitive glucose transport; adenylate cyclase responsiveness to parathyroid, but not to antidiuretic, hormone). These cells thus help us to identify the toxicological effects of Corexit on adult kidney cells. Previous studies have tested the Corexit toxicity in liver cell lines (Judson et al., 2010), but so far no reports have been published for the kidney cell toxicity.

To evaluate Corexit toxicity on human kidney cells, we incubated HK2 and HEK 293 cell lines with different concentrations of Corexit (20, 40, 80, 160, and 200 ppm) for 48 hours in both serum-free and serum-fed media. Results showed that HK-2 cells shares H19-7 cell's less sensitivity towards Corexit induced cell death under serum-fed conditions. Only, 20% of cell death was observed in serum-fed states at the highest concentration of Corexit. On the other hand, in serum-free states Corexit caused cell toxicity was prominent with 160 ppm of Corexit resulting in 80% cell death (see Figure 2-12 and Figure 2-13). These results imply that Corexit can disrupt normal kidney functions at higher concentrations and thus can result in kidney failure

that can, if not treated well, lead to other systemic problems. The LC50 of HK2 cell was 95 ppm, the LC50 of HEK 293 was 93 ppm.

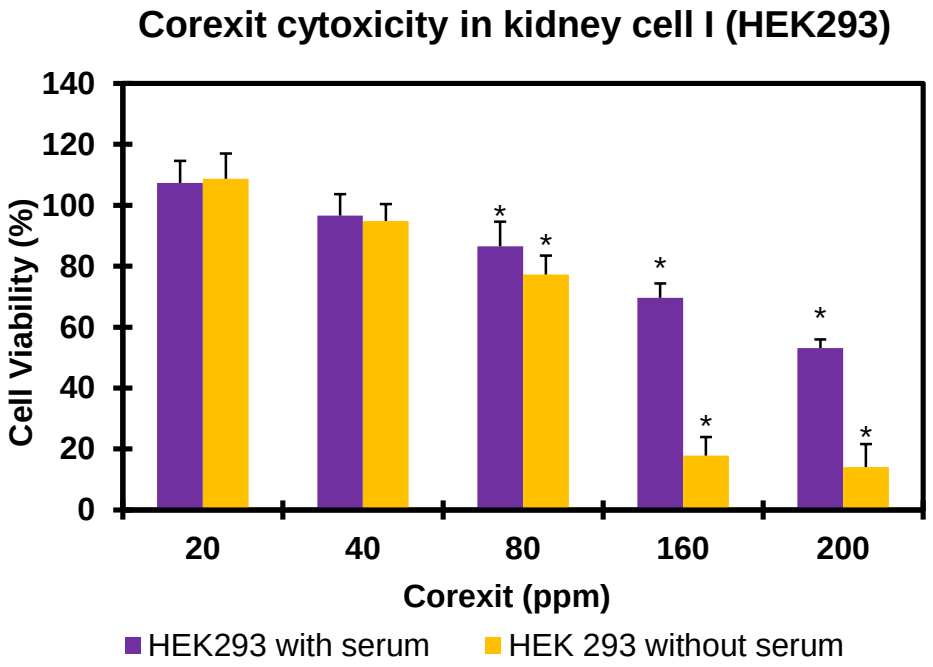

Figure 2-12 Effects of Corexit on kidney cell-I

Cells were treated with different concentration of Corexit for 48 hours. At the end of incubation period, the MTT assay was performed to assess the cell viability. The percentage of cell viability was calculated by dividing the reading of the target well to the control. Control cells were incubated in Corexit free media run in parallel to treatment groups. The data are expressed as mean ± of three independent experiments (duplicates in each experiment). (*) indicates a statistically significant difference compared to controls ($p<0.005$).

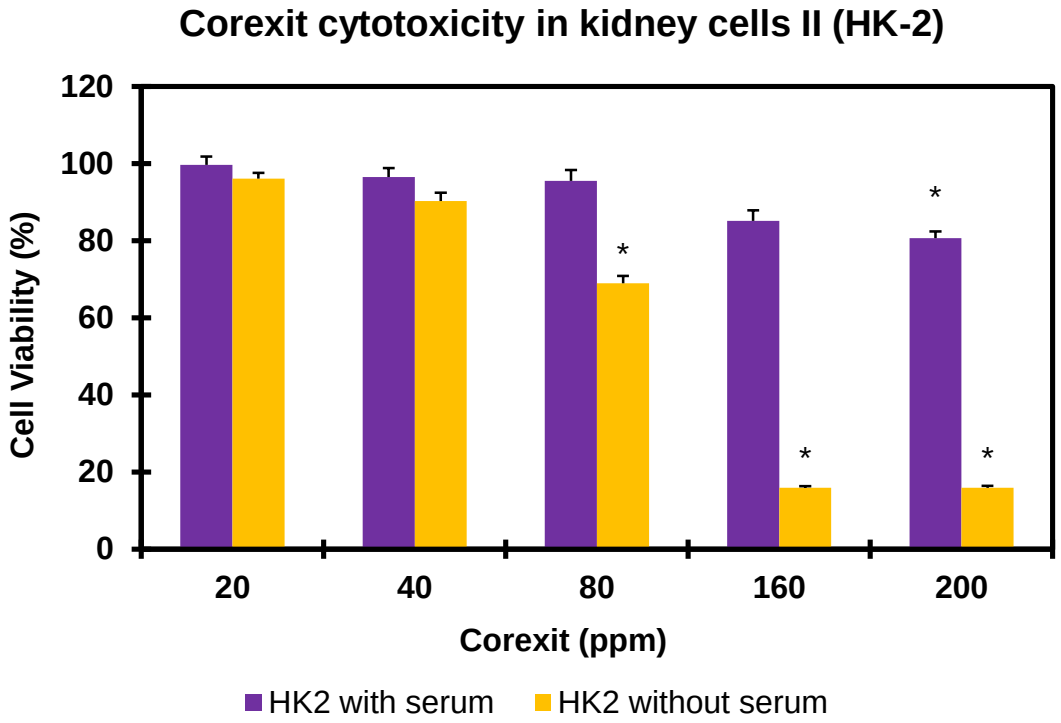

Figure 2-13 Effects of Corexit in kidney cell-II.

Cells were treated with different concentration of Corexit for 48 hours. At the end of incubation period, the MTT assay was performed to assess the cell viability. The percentage of cell viability was calculated by dividing the reading of the target well to the control. Control cells were incubated in Corexit free media run in parallel to treatment groups. The data are expressed as mean ± of three independent experiments (duplicates in each experiment). (*) indicates a statistically significant difference compared to controls ($p<0.005$).

2.3 Discussion

In this study, we have investigated the effect of Corexit under two types of cell metabolic conditions. One with a normal amount of growth factors (i.e. serum-fed media), and another at a relatively compromised state where the cells have limited or no access to growth factors present in the serum (i.e serum-free media). The serum-free media indirectly represents a compromised

state of organs and a body system. Previous reports have already established that MTT based cell proliferation assay is conspicuously dependent on the metabolic state of cells. Vistica et al. (1991) has shown that the MTT assay is significantly influenced by the growth factor concentration in the DMEM medium. The differences in MTT reduction in relation to medium type may be attributable to the protein concentrations provided by FBS or FS in the media. In our study, we found that different cells have different ability to resist the toxicity of Corexit. Under serum-free conditions, the order of sensitivity towards Corexit induced cell death was found to be: B16/BL6 > 1321N1 > H19-7 > HEK293 > HK2. The average value of LC50 for each cell line was found to be: 16 ppm for BL16/B6; 33 ppm for 1321N1; 70 ppm for H19-7 cell; 93 ppm for HEK 293 CELL; and 95 ppm for HK2 cell. These results imply that highly proliferative cells were found to be more susceptible to Corexit induced cell death as compared to normally transformed adult cells of neuronal and kidney tissues. More studies are needed to understand the toxicity mechanisms

CHAPTER 3. Understanding toxicity mechanisms

3.1 Introduction

Cell death can be categorized into either apoptosis or necrosis (Edinger and Thompson, 2004). Apoptosis, also known as programmed cell death nuclear involves condensation, fragmentation and cleavage of chromosomal DNA without causing inflammation. Necrosis involves the breakdown of the plasma membrane, followed by release of cellular contents which potentiates inflammation around the dead cell. Figure 3-1 shows microscopically, cellular death by (a) apoptosis and (b) necrosis. The objective of current study was to develop a fundamental understanding of Corexit toxicity mechanisms at the cellular level. We hypothesize that the cytotoxicity of Corexit involves apoptosis, necrosis, oxidative stress, and mitochondria dysfunctions. We test this by quantifying different toxicity markers.

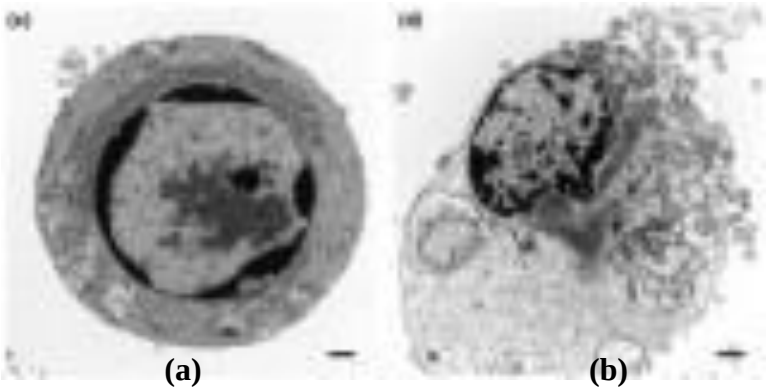

Figure 3-1 (a) Apoptosis in a cell, (b) Necrosis in a cell

(Edinger and Thompson, 2004)

Our primary interest was to evaluate the role of reactive oxygen species (ROS) in Corexit mediated toxicity. ROS refers to free radicals such as hydroxyl (·OH), alkoxyl (RO), and peroxyl (ROO) radicals, and it also includes non-radicals such as hydrogen peroxide (H_2O_2). ROS can be formed from the by-products of reactions affecting the electron transportat chain (ETC) in the mitochondria (Wolfe et al. , 2001). The ETC serves as the means of oxidative phosphorylation in eukaryotes. Figure 3-2 shows the transport of electrons between the

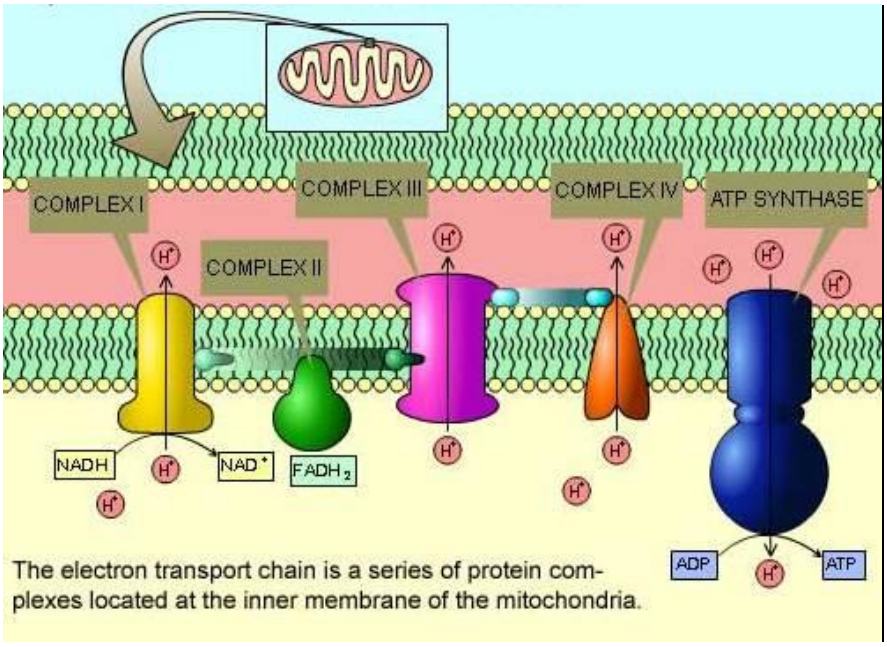

Figure 3-2 Electron Transpiration Chain (Liou, 2011)

mitochondrial complexes, which results in the formation of a proton concentration gradient across the mitochondrial membrane. (Note protons are pumped by the ATP synthase to produce ATP from ADP). However, during this process, electrons can leak from the chain and form superoxide anion (O_2^-) (Passos and Von Zglinicki, 2006). Superoxide anion is believed to be the first oxidation and reduction reaction product in ETC. The superoxide anion formation in the ETC occures within complex-I and complex-III. Previous studies have mapped the potential relation between Complex-I and ROS (Beers and Sizer, 1952).

As shown in Figure 3-3, under normal conditions, the superoxide anion will be converted to hydrogen peroxide by superoxide dismutase (SOD) (Passos and Von Zglinicki, 2006). There are different kinds of SODs, manganese superoxide dismutase (Mn-SOD), which exists within the mitochondria and copper-zinc superoxide dismutase (CuZn-SOD), located in the cytosol (Green and Reed, 1998). The dismutation of superoxide radicals into hydrogen peroxide and oxygen is an important mechanism for the protection of cells against the damage from superoxide radicals. Hydrogen peroxide is a very unstable molecule and thus it will be reduced by ferrous ions in the cell to form and hydroxyl radicals (·OH), a process known as the fenton reaction (Winterbourn, 1995):

$$Fe^{2+} + H_2O_2 \longrightarrow Fe^{3+} + OH\cdot + OH^-$$

When ROS are generated in the cell, antioxidants such as glutathione and catalase will be produced as a self-protective mechanism (Passos and Von Zglinicki, 2006, Simon et al., 2000). The imbalance between prooxidant and antioxidant can cause accumulation of ROS. ROS have detrimental effects on mitochondria, protein, lipids and DNA, as shown in Figure 3-3. Increased concentration of ROS can result in cell death (Simon et al., 2000).

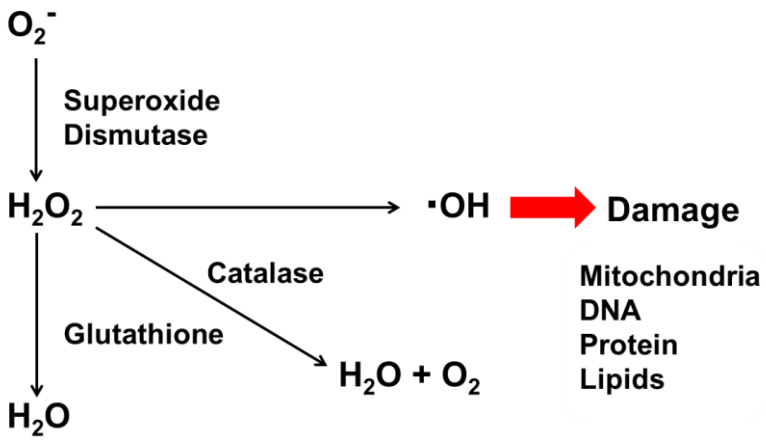

Figure 3-3 Formation of reactive oxygen species

Hydroxyl radicals can attack the cell membrane and initiate lipid peroxidation. During the early stage of cell death, DNA strand breakage occurs. The permeability of the cell membrane will increase due to the increased generation of calcium ion in the cell, concurrently specific proapoptotic and antiapoptotic protein will be expressed (AC Andreazza et al., 2010). Development of lipid peroxidation is another highly significant effect during the development of apoptosis associated with ROS formation.

Researchers have shown that apoptosis is initiated from different pathways (Schulze-Osthoff et al., 1993). It is generally accepted that neurodegenerative diseases (e.g. Alzheimer) are related to neuronal apoptosis (Shimohama, 2000). The role of mitochondria in cellular apoptosis generally falls into three categories: first, when cells are under stress, the disruption of electrons from the electron transportation chain (ETC) is recognized as an early feature for cell death. Second, under these conditions, capase-activiting proteins (e.g. caspase 9) would increase. Third, under some selected forms of stress, cellular redox potential is altered due to the imbalance in the production of radical scavenging enzymes (Adler et al., 1999).

During the DWH oil spill event, over 4800 workers were involved in various clean-up efforts (Castranova, 2011). The Corexit 9500 and Corexit 9527 were applied by airplane. Those workers on site were at risk for exposure mainly via inhalation. Such inhaled fractions might potentially permeate or translocate to the brain via the olfactory or systemic circulation, therefore producing central nervous system (CNS) abnormalities. The vapor pressure of Corexit is less than 5 mm Hg at 38 ˚C (NALCO, 2010). This implies Corexit can enter into the olfactory system by inhalation, and may have the potential to cross blood brain barrier and cause central nervous system dysfunctions. To better understand the toxic effects of Corexit upon the brain, we utilized an in vitro cellular methodology by utilizing hippocampal neuronal (H19-7) cells.

3.2 Materials and Methods

3.2.1 Mitochondrial complex-I activity

Mitochondrial complex-I activity (NADH dehydrogenase activity) is based on the NADH oxidation. Oxidation of NADH by the NADH-dehydrogenase enzyme present in the tissue homogenate was measured spectrophotometrically at 340 nm. The cell homogenate was added to the reaction mixture containing NADH, coenzyme Q10 and phosphate buffered saline. To analyze its effect on NADH, oxidation was monitored by measuring the decrease in absorbance at 340 nm. The change in absorbance would indicate the amount of NADH oxidized. Results were expressed as percentage control.

3.2.2 Determination of reactive oxygen species generation

Reactive oxygen species (ROS) generation in the cell treated with Corexit was estimated by spectro-fluorometerically detection of conversion of non-fluorescent chloromethyl-DCF-DA (2' ,7- dichlorofluorescin diacetate, DCF-DA) to fluorescent DCF at an excitation wavelength of 492 nm and at an emission wavelength of 527 nm. 0.0005% w/v solution of DCF-DA in ethanol (10 ul), phosphate buffer (280 ul) and cell homogenate (10 ul) were incubated for 1 hour at 37°C. DCFH reacted with ROS to form the fluorescent product DCF. Intensity was analyzed by BioTek Synergy HT plate reader (BioTek, VT, USA). Results were expressed as percentage control.

3.2.3 Superoxide dismutase activity

When ROS are generated in the cell, antioxidants (superoxide dismutase, catalase, glutathione) will be generated as a self-protection mechanism. The superoxide dismutase activity was measured by using the HT Superoxide Dismutase Assay purchased from TREVIGEN. In this assay, a fixed amount of superoxide radicals was generated from conversion of xanthine to

uric acid and hydrogen peroxide by xanthine oxidase. The generated superoxide radicals converted WST to WST-1 formazan, which absorbed light at 450 nm. SOD levels were determined by measruing the amount of superoxide radicals generated by the conversion of xanthine to uric acid would decrease, whom leads to the reduced amount of WST-1 formazan that would quantify the reduced absorbance.

3.2.4 Estimation of catalase

Catalase activity was assayed by the Beer and Sizer method (Beers and Sizer, 1952). The assay mixture consisted of 260 ul of 30 mM solution of hydrogen peroxide in phosphate buffer (0.05 M, pH 7.0), and 40 µl of cell homogenate in a final volume of 300 uL. Solution of hydrogen peroxide was added last since the reaction of hydrogen peroxide degradation was very fast. Hydrogen peroxide without tissue homogenate was used as blank. Change in absorbance was recorded at 240 nm for 2-3 minutes. Catalase activity was calculated as change in absorbance at 240 nm (ΔA240/min) from the initial (45 second) linear portion of the curve. Results were expressed as percentage control.

3.2.5 Glutathione estimation

GSH was measured fluorimetrically as described earlier by Cohn and Lyle (1966). Principally, this method employs o-phthalaldehyde (OPT) condensation reaction with GSH to yield a fluorescent product at pH 8.0. Briefly, assay mixture consisted of 0.1% OPT solution in methanol (100 ul), 0.01M phosphate buffer (1.8 ml) and supernatant of tissue (100 ul) after precipitation of protein by 0.1M phosphoric acid treatment. The assay mixture was incubated for 20 minutes and readings were taken at excitation and emission wavelengths of 340 and 420 nm, respectively. A standard curve was prepared from commercially obtained GSH. The GSH

content was calculated as mmol of GSH/µg protein and were reported as percentage control levels.

3.2.6 Estimation of lipid peroxidation

The index of lipid peroxidation was estimated by measuring the malondialdehyde (MDA) content in the form of thiobarbituric acid-reactive substances according to the method of Ohkawa et al. (1979). Briefly, 100 µl of cell homogenate and 200 µl ice cold TCA (10% w/v in double distilled water) were incubated for 15 minutes on ice. Assay mixture was centrifuged at 2200g for 15 min at 4°C temperature. Placed 200 µL supernatant of standards and samples into new labeled screw top 1.5 ml tubes and equal volumes (200 µL) of 0.67% TBA was added. The reaction mixture was incubated for 20 minutes in boiling water. Samples collected after incubation were cooled down to room temperature and placed in 96-well plate. A standard curve of TBARS reactive substances was also prepared by employing different concentrations of MDA. Absorbance was read in a plate reader at 532 nm and MDA levels were calculated as TBARS reactive substances per mg of protein. Results were expressed as percentage control.

3.3 Results and Discussion

3.3.1 Complex-I activity

Complex-I and Complex-III are the two main sites in respiration chain, where oxygen molecular are converted to superoxide anions (Turrens, 1997). Researches have shown the compromised Complex-I activity is related to the increased generation of superoxide anion (Pitkanen and Robinson, 1996). Also, the inhibition of Complex-I activity can relate to the dysfunction of mitochondria, leading to apoptosis or necrosis. Many neurodegenerative diseases like Parkison's disease are related to decreased Complex-I activity (Lu and Finkel, 2008, Shaw et

al., 2002). During the DWH oil spill, most of the Corexit was applied by airplanes; the vapor pressure of Corexit is low, and therefore Corexit can cross the blood brain barrier and enter into the central nervous system (Sriram et al., 2011). A previous study has shown the inhalation of Corexit caused olfactory dysfunction in mammalian animals (Sriram et al., 2011). In this study, we use neuronal cells (H19-7) to test whether Corexit has the potential to cause the inhibition of Complex-I activity.

Figure 3-4 shows, a toxic dosage of Corexit (80 ppm) significantly decreased the Complex-I activity in neuronal cells, suggesting Corexit may lead to reduced generation of ATP and might hamper normal function of ETC. This could generate of superoxide anions in the cells.

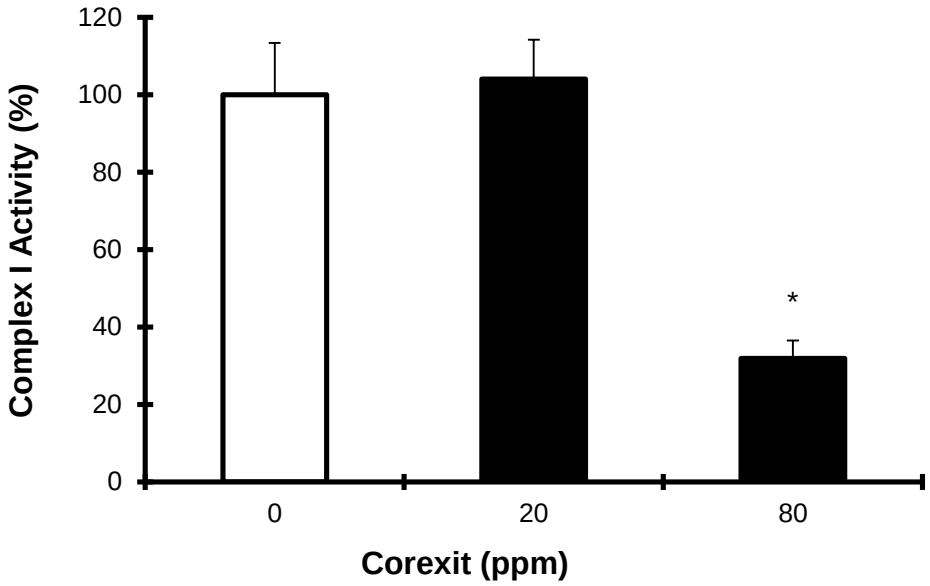

Figure 3-4 Effects of Corexit (20ppm, 80ppm) on mitochondrial Complex I activity in neuronal cells (H19-7 cells).

Corexit (80ppm) showed siginificantly decreased Complx I activity ($n=6$, $p<0.005$) as compared to control.

3.3.2 Reactive oxygen species activity

Measuring the superoxide anions generated in cellular systems is a difficult task due to the high reactivity and short half-life nature of the superoxide anions (Rapoport et al., 1994). When a superoxide anion is generated in a system, an enzyme called superoxide dismutase (SOD) can convert superoxide anion to hydrogen peroxide (Passos and Von Zglinicki, 2006). Hydrogen peroxide is not a stable molecule and it forms hydroxyl radicals through fenton reaction (Winterbourn, 1995). Superoxide anion, hydrogen peroxide and hydroxyl radical are all ROS species which can damage the cell directly or indirectly (Wallace and Melov, 1998). Therefore, we measured ROS species in the cell. In the ROS assay, DCFH-DA, a non-ionic chemical substance, crosses the cell membrane and is hydrolyzed by intracellular esterases to nonfluorescent DCFH, the DCFH will be converted into high fluorescent DCF by ROS (Andreazza et al., 2010).

Figure 3-5 shows ROS generation in Corexit treated cells in H19-7 cell line. Two concentrations of Corexit were selected. Corexit at 20 ppm represents the non-toxic dosage, while Corexit at 80 ppm represents the concentration which causes 50 percent cell death (LC50). Our data show 20 ppm Corexit increased the ROS generation by approximately 10% when compared to the control. Furthermore, 80 ppm Corexit exhibited considerable increase in ROS ($n=6$, $p<0.005$). These data indicate that the cells are under conditions of high stress when exposed to Corexit, and could result in Corexit induced cell death. Wilk et al. (2013) have demonstrated that nontoxic dosage of polycyclic hydrocarbons can trigger ROS generation and cause oxidative DNA damage. Bandele et al. (2012) reported ROS increased 4.5 fold (compared with the control) after 24 hours of incubation with Corexit 9500 (100 ppm) on HepG2/C3A cell, while DOSS dramatically increased the ROS by 5 fold under the same dosage and condition.

This suggests the ROS generation from DOSS could play a vital role in Corexit induced cytotoxicity effects.

ROS can cause damage to proteins, lipids, and mitochondria thereby causing cell death (Cabiscol et al., 2000). However, evidence to determine which ROS mainly involved in the reaction remains inconclusive. It has been shown that neither superoxide anion nor hydroxyl radicals are directly involved in the oxidation of DCFH. While the oxidants formed during the reduction of hydrogen peroxide and peroxidase may oxidize the DCFH (Andreazza et al., 2010).

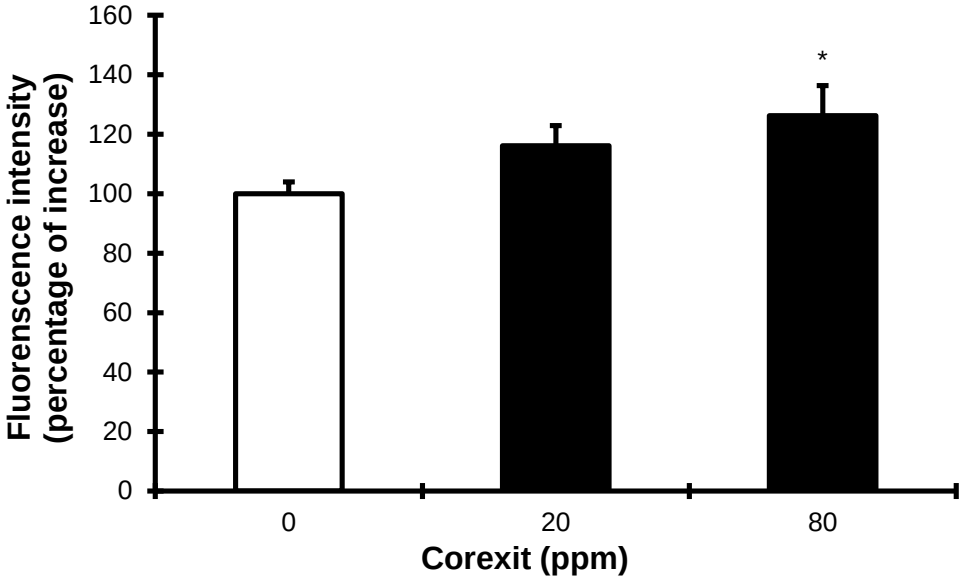

Figure 3-5 Effects of Corexit (20ppm, 80ppm) on reactive oxygen species in neuronal cells (H19-7 cells).

Corexit (80ppm) caused significant generation of reactive oxygen speices ($n=6$, $p<0.005$) as compared to control.

3.3.3 Superoxide dismutase, catalase, glutathione effects

Superoxide radicals are associate with neurodegenerative diseases, ischemia reperfusion injury, atherosclerosis, and aging (Lu and Finkel, 2008). When superoxide anion is produced, the self-protection mechanism in the cell generates antioxidants to protect the cell from deleterious effects. We tested the activities of antioxidant superoxide dismutase enzyme (SOD), catalase enzyme (CAT), and glutathione content (GSH) in Corexit treated H19-7 cells. Figure 3-6 indicates that the activity of SOD did not change after the cells were treated with 20 ppm of Corexit for 48 hours, while the cells treated with 80 ppm of Corexit showed significant ($n=6$, $p<0.005$) increase in SOD activity. These data suggests that 80 ppm of Corexit has triggered cellular defense against the oxidative injury caused by the generation of ROS.

In Figure 3-6 we can observe increased, but not significant, SOD activity in the cells treated with 20 ppm of Corexit after 48 hours. However, significant SOD activity ($n=6$, $p<0.005$) was found in cells treated with 80 ppm of Corexit after 48 hours. The data indicated superoxide anion was converted to hydrogen peroxide by SOD.

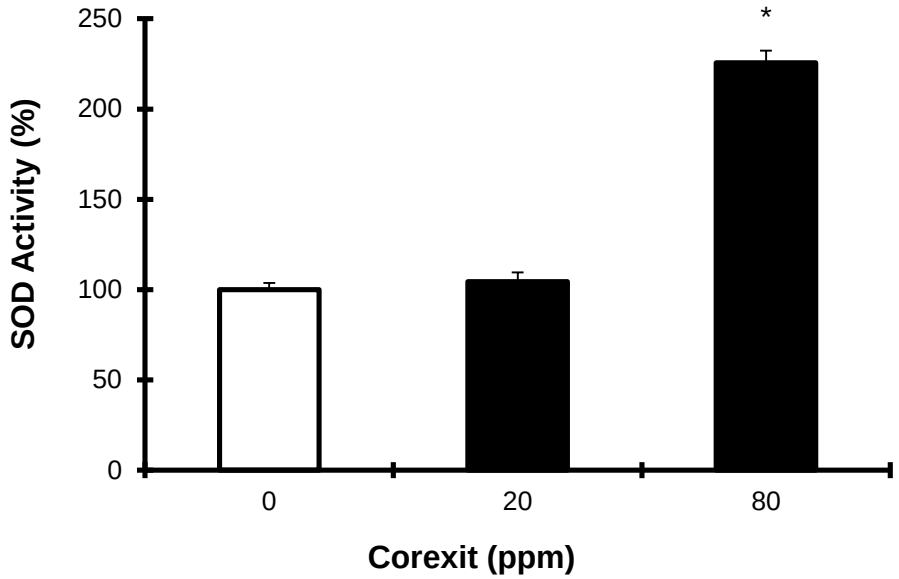

Figure 3-6 Effects of Corexit (20ppm, 80ppm) on SOD activity in neuron cells (H19-7 cells)

Corexit (80ppm) caused significant increase of SOD activity ($n=6$, $p<0.005$) as compared to control.

Catalase enzyme could directly scavenge hydrogen peroxide to form water and oxygen, therefore can protect the cell from the deleterious effects of hydrogen peroxide (Shirahata et al., 1997). Figure 3-7 shows a significant catalase activity in cells treated with 80 ppm Corexit ($n=6$, $p<0.005$). While cells treated with 20 ppm Corexit show a slight increase in catalase activity.

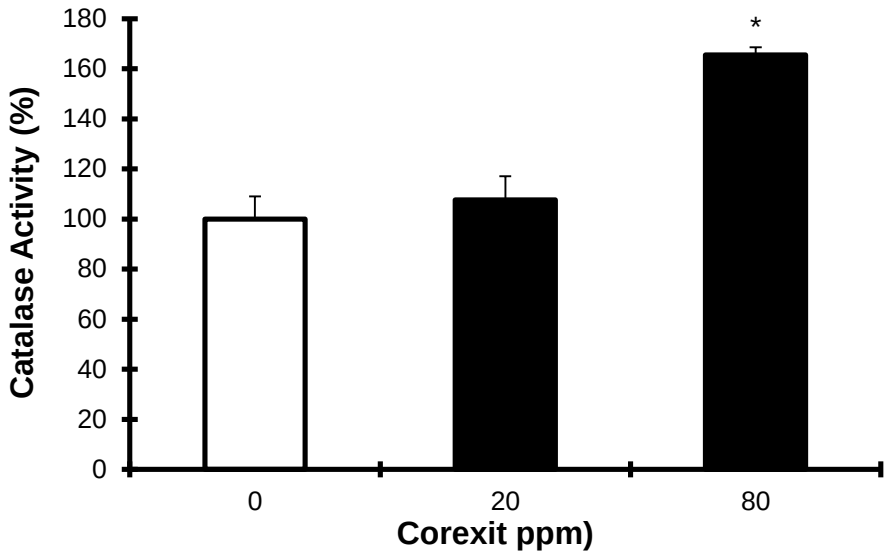

Figure 3-7 Effects of Corexit (20ppm, 80ppm) on catalase activity in neuronal cells (H19-7 cells).

Corexit (80ppm) caused significant increase of catalase activity ($n=6$, $p<0.005$) as compared to control.

Figure 3-8 shows when the cells were treated with 20 ppm of Corexit for 48 hours, there was a slight decrease of GSH, however cells treated with 80 ppm Corexit showed significant ($n=6$, $p<0.005$) depeletion of GSH. GSH plays a vital role in cellular metabolism as an antioxidant and radical scavengers. It is commonly believed that the depletion of GSH may lead to oxidative stress (Mytilineou et al., 2002), and the decreased cellular GSH level is associated with ROS-mediated apoptosis (Circu and Aw, 2010).

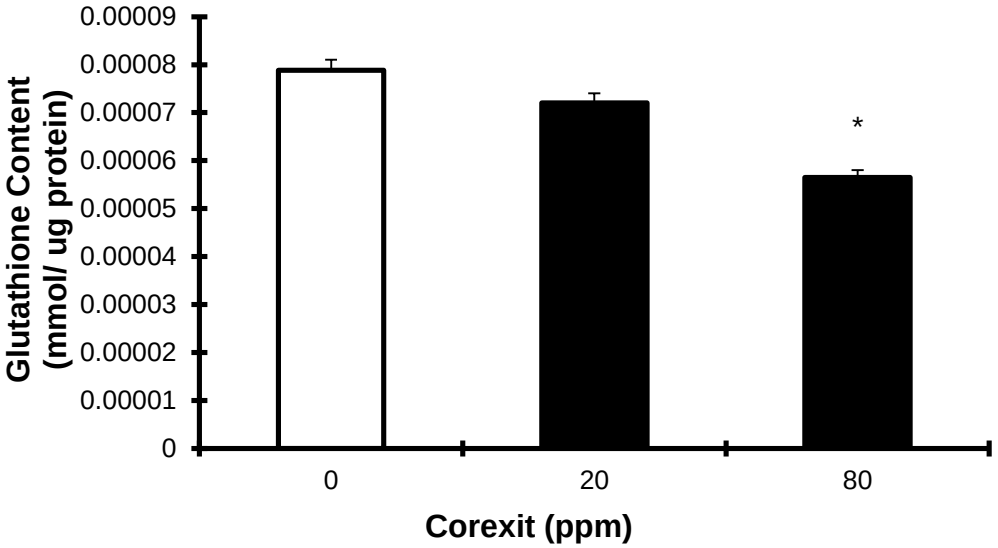

Figure 3-8 Effects of Corexit (20ppm, 80ppm) on GSH content in neuron cells (H19-7 cells). Corexit (80ppm) caused significant depletion of GSH content (n=6, $p<0.005$).

3.3.4 Lipid peroxidation

Among all the reactive oxygen species, hydroxyl radicals are the most active; hydrogen peroxide and superoxide anion are not as detrimental as hydroxyl radical. If the hydroxyl radical exists, it will cause damage to the mitochondria, DNA, and cell membrane (Cabiscol et al., 2000). The lipid peroxidation assay was used to find out whether there was degradation of lipids in the cell, thereby serving as an indicator of damage to cell membrane. Figure 3-9 shows that cells treated with 80 ppm Corexit showed significant (n=6, $p<0.005$) level of lipid peroxide. Oxidative stress caused by the generation of ROS can damage many biological molecules; lipid peroxidation occurs late in the injury process, while proteins and DNA are more significant targets of ROS (Halliwell and Chirico, 1993). Our data indicate Corexit caused the degradation of lipids on the cell membrane and this damage occurred late in the injury process.

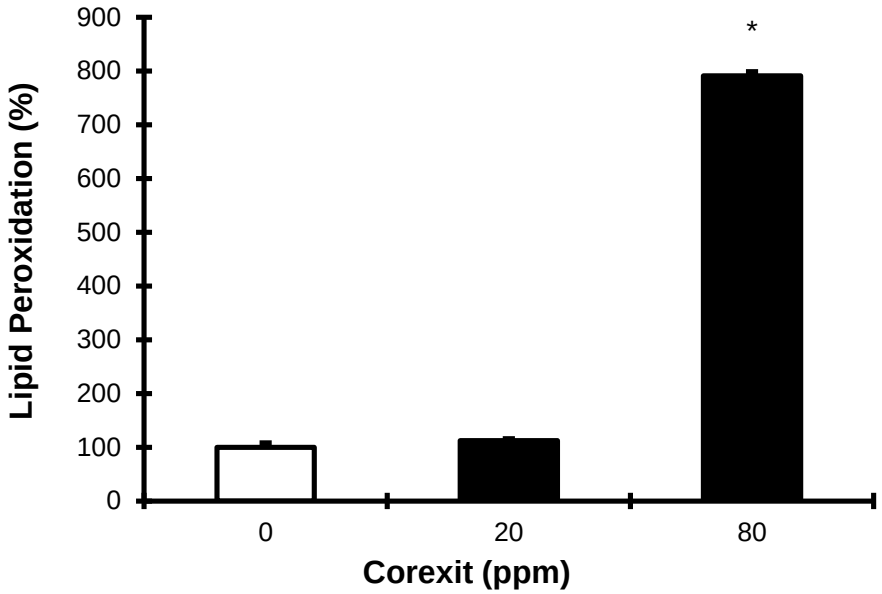

Figure 3-9 Effects of Corexit (20ppm, 80ppm) on lipid peroxide in neuronal cells (H19-7 cells).

Corexit (80ppm) caused significant increase in lipid peroxidiation ($n=6$, $p<0.005$) as compared to control.

3.4 Discussion

Unlike natural disasters such as hurricanes and earthquakes, oil spills can negatively affect ecosystems years after the event. Apart from affecting the neighboring ecological niches, oil spills can impact several aspects of human activities. The Exxon Valdez oil spill (EVOS), which occurred in Prince William Sound, Alaska, on March 24, 1989, revealed that in addition to affecting sea birds and marine animals, the spill also impacted socio-economic conditions of people residing in nearby areas (Goldstein et al., 2011). Alaska oil spill caused economic losses for fishermen and supporting businesses, increased social conflict, fostered declines in community cohesiveness, and lead to alcohol and drug abuse in some of the local populations (J. Steven Picou, 1992). Additionally, oil spill events such as the DWH oil spill lead to a large-scale

environmental contamination that impacts the recreational and ecological value of the entire ecosystem (Hayworth, 2011, Hayworth and Clement, 2011).

Cell-based toxicity models can provide a sensitive and reliable toxicity assessment, while avoiding complications arising through the use of conventional animal-based toxicological screening studies (Bandele et al., 2012). Biologically relevant endpoints and biomarkers can be used to deduce the toxicity of complex mixtures and to identify the constituent(s) that may adversely affect the physiological activities. The advantages of these toxicological systems include accumulating accurate and valuable information over a short time interval, which can assist in the development of further experimental strategies. In our study, we found that different mammalian cells have variable ability to resist Corexit toxicity effects. Cells were found to be more defenseless under serum-free states when compared to serum-fed states. In the serum-free state, the order of sensitivity towards Corexit induced cell death was found to be: B16/BL6 > 1321N1 > H19-7 > HEK293 > HK2. The average value of LC50 for each cell line was found to be: 16 ppm for BL16/B6; 33 ppm for 1321N1; 70 ppm for H19-7 cell; 93 ppm for HEK-293 and 95 ppm for HK-2 cell. These results imply that highly proliferative cells are more susceptible to Corexit induced cell death, as compared to normally transformed adult cells of neuronal and kidney tissues. Previous studies have reported the LC50 of Corexit in two human liver cell lines (HepG2 and HepG2/C3A) to be 120 ppm and 250 ppm, respectively (Judson et al., 2010).

Since part of the dispersant (Corexit) was applied by the aerial route (spraying from airplanes), on site workers could have inhaled the dispersant mist and their skin could have been directly affected by the dispersant. Due to inhalation, the respiratory tract could have been affected and also the inhaled Corexit mist could have affected the central nervous system. Corexit due to its lipophilicity can cross the blood brain barrier and permeate the brain through

the olfactory system and influence the neurons and the glial cells. In several in vivo studies, scientists have exposed animals (rats) to Corexit (sprayed 27mg/m^3 for 5 hours) by nasal route (Roberts et al. , 2011, Sriram et al. 2011, Anderson et al. (2011) and found it to affect the CNS and other organs of the animal. Corexit can also enter the systemic circulation by permeating through the dermal route. By successfully entering the systemic circulation, Corexit can affect several organs, tissues and cells in the human body. Thus, Corexit can be potential environmental and occupational hazard.

In the current study, our aim was to develop a fundamental understating of Corexit toxicity at the cellular level. The data obtained from this study will be useful for quantifying the environmental and human health risks posed by Corexit. Furthermore, the result obtained from this study will help to understand the underlying toxicity mechanisms which can be used to develop novel drug therapies to protect against Corexit-induced toxicity effects. Mechanistically, the electron transportation chain serves as the means of oxidative phosphorylation in eukaryotes. Through electron transportation chain, ATP is produced to provide the energy for living cells and this procedure occurs on the membrane of the mitochondria. The decreased activity of Complex-I can lead to the dysfunction of mitochondria. Previous studies have mapped the potential relation between Complex-I and ROS generation (Beers and Sizer, 1952). ROS includes free radicals such as hydroxyl (·OH), alkoxyl (RO), and peroxyl (ROO) ions, it also includes non-radicals such as hydrogen peroxide (H_2O_2). ROS are the by-products of electron transportation chain reactions in the mitochondria (Wolfe et al., 2001). And it is believed that the generation of superoxide anion is related within Complex-I and Complex-III (Beers and Sizer, 1952). When superoxide anion is formed, the superoxide dismutase will be activated and convert superoxide anion to hydrogen peroxide. Glutathione and catalase are the two antioxidants which can

eliminate the deleterious effects of hydrogen peroxide by converting it to water and oxygen. If formed in excess, Hydrogen peroxide being a stable chemical will be rapidly degraded to OH·. The hydroxyl radical thus formed attacks cell membrane and initiate lipid peroxidation, causing DNA cleavage, and protein degradation.

Our results show decreased Complex-I activity in cells treated with Corexit (80ppm) which indicated mitochondria dysfunction. ROS concentrations increased significantly after cells were treated with Corexit (80ppm) for 48 hours, indicating that the cells were under stressful conditions. Meanwhile, the antioxidants also responded to the stress triggered by Corexit. The SOD activity was elevated indicating a self-protection mechanism of the cell, while catalase activity was also increased. However, another antioxidant GSH showed decreased activity in cells treated with high concentration of Corexit (80ppm). It has been reported in the published literature that the depletion of GSH may be the reason for accumulation of ROS within cells (Sakon et al., 2003). Our data is consistent with this literature data since we also observed increased level of ROS and decreased level of GSH, indicating Corexit induced depletion of GSH. The significant increased LPO activity in cells treated with Corexit (80ppm) suggests the lipids on the surface of the cell membrane were degraded; and this could explain cell death. The apoptotic maker Caspase-3 and Bax was also shown to increase in response to toxic levels of Corexit (at 80 ppm). Overall, our experimental data support our hypothesis that Corexit induced cell death was caused by apoptosis.

CHAPTER 4. Conclusion and future work

Using the cell viability assay (MTT-based), we have shown that highly proliferating cells are more susceptible to Corexit-induced toxicity. Corexit at higher concentrations appears to be a potential neuronal and nephron toxin. We hypothesize that this toxic effect will be more pronounced when crude oil is mixed with Corexit and our ongoing research will address this hypothesis. Based on our current study, Corexit exhibits its toxicity by inducing oxidative stress, mitochondrial dysfunction, and apoptosis. Hence, use of antioxidants and mitochondrial energy enhancers could potentially decrease both acute and chronic toxicity effects of Corexit.

In future work the toxicity of Corexit and oil combination or water accommodated fraction (WAF) of Oil-Corexit mixtures may need to be investigated. The *in vitro* toxicity cannot be a replacement for an *in vivo* study. Few studies reported the toxicity of Corexit, oil and WAF on a mammalian animal's body (Anderson et al., 2011). The whole animal study of Corexit, oil, and WAF toxicity can help to study the metabolism pathways of these potential toxins and increase our understanding of the toxicity mechanisms.

There is limited research available about the bioaccumulation effects of Corexit in marine animals. Although oil and Corexit concentrations in the marine species in Gulf shore have been quantified after the oil spill, bioaccumulation and biomagnification are long-term effects that can only be detected in a long run. It is recommended that a long term monitoring system be established in the near shore environment to track ambient Corexit and oil concentrations in water and also in various marine species.

CHAPTER 5. Reference

AC Andreazza, L Shao, J Wang, Young L. MItochondrial complex i activity and oxidative damage to mitochondrial proteins in the prefrontal cortex of patients with bipolar disorder. Archives of General Psychiatry. 2010;67:360-8.

Adler V, Yin Z, Tew KD, Ronai Z. Role of redox potential and reactive oxygen species in stress signaling. Oncogene. 1999;18:6104-11.

Ahlers J, Cascorbi I, Foret M, Gies A, Kohler M, Pauli W, et al. Interaction with functional membrane proteins--a common mechanism of toxicity for lipophilic environmental chemicals? Comp Biochem Physiol C. 1991;100:111-3.

Anderson SE, Franko J, Lukomska E, Meade BJ. Potential Immunotoxicological Health Effects Following Exposure to COREXIT 9500A during Cleanup of the Deepwater Horizon Oil Spill. Journal of Toxicology and Environmental Health, Part A. 2011;74:1419-30.

Andreazza A, Shao L, Wang J, Young L. MItochondrial complex i activity and oxidative damage to mitochondrial proteins in the prefrontal cortex of patients with bipolar disorder. Archives of General Psychiatry. 2010;67:360-8.

Atlas RM. Petroleum biodegradation and oil spill bioremediation. Marine Pollution Bulletin. 1995;31:178-82.

ATSDR. Yellowstone River 2011: Silvertip Pipeline Spill Light Crude Oil Information for Health Professionals. 1999.

Bandele OJ, Santillo MF, Ferguson M, Wiesenfeld PL. In vitro toxicity screening of chemical mixtures using HepG2/C3A cells. Food and Chemical Toxicology. 2012;50:1653-9.

Barnes D, Sato G. Serum-free cell culture: a unifying approach. Cell. 1980;22:649-55.

Barron MG, Ka'aihue L. Critical evaluation of CROSERF test methods for oil dispersant toxicity testing under subarctic conditions. Marine Pollution Bulletin. 2003;46:1191-9.

Bartha R, Atlas RM. Biodegradation of oil on water surfaces. Google Patents; 1976.

Beers RF, Sizer IW. A spectrophotometric method for measuring the breakdown of hydrogen peroxide by catalase. J Biol Chem. 1952;195:133-40.

Berridge MV, Horsfield JA, Tan AS. Evidence that cell survival is controlled by interleukin-3 independently of cell proliferation. J Cell Physiol. 1995;163:466-76.

Bianchi V. Nucleotide pool unbalance induced in cultured cells by treatments with different chemicals. Toxicology. 1982;25:13-8.

Blumer M. Oil Pollution. Persistence and degradation of spilled fuel oil, Science. 1972;176:1120-2.

Bobra AM, Shiu WY, Mackay D, Goodman RH. Acute toxicity of dispersed fresh and weathered crude oil and dispersants to Daphnia Magna. Chemosphere. 1989;19:1199-222.

Bourdeau P. Short-term toxicity tests for non-genotoxic effects: Wiley; 1990.

Cabiscol E, Piulats E, Echave P, Herrero E, Ros J. Oxidative Stress Promotes Specific Protein Damage inSaccharomyces cerevisiae. Journal of Biological Chemistry. 2000;275:27393-8.

Castranova V. Bioactivity of Oil Dispersant Used in the Deepwater Horizon Cleanup Operation. Journal of Toxicology and Environmental Health, Part A. 2011;74:1367-.

Circu ML, Aw TY. Reactive oxygen species, cellular redox systems, and apoptosis. Free Radical Biology and Medicine. 2010;48:749-62.

Clark JR, G.E. Bragin, R.J. Febbo and D.J. Letinski. . Toxicity of physically and chemically dispersed oils under continuous and environmentally realistic exposure conditions: Applicability to dispersant use decisions in spill response planning. In Proceedings of the 2001 International Oil Spill Conference, Tampa, Florida American. 2001:1249-55.

Clayton JR, Payne JR, Farlow JS. Oil Spill Dispersants: Mechanicsms of Action and Laboratory Tests: C.K. Smoley; 1993.

Clement TP, Hayworth JS, Mulabagal V, Yin F, John GF. Research Brief II: Impact of Hurricane Isaac on Mobilizing Deepwater Horizon Oil Spill Residues along Alabama's Coastline – A Physicochemical Characterization Study. 2012.

Coelho G, Clark J, Aurand D. Toxicity testing of dispersed oil requires adherence to standardized protocols to assess potential real world effects. Environ Pollut. 2013;177:185-8.

Cohn VH, Lyle J. A fluorometric assay for glutathione. Anal Biochem. 1966;14:434-40.

Cohrssen JJ, Covello VT, Quality CoE. Risk analysis: a guide to principles and methods for analyzing health and environmental risks: Executive Office of the President of the U.S., Council on Environmental Quality; 1989.

Commer M. Chemical Dispersants and You: What It's All About. 2010.

Costa M. Levels of ornithine decarboxylase activation used as a simple marker of metal induced growth arrest in tissue culture. Life Sci. 1979;24:705-13.

Cui D, Tian F, Ozkan CS, Wang M, Gao H. Effect of single wall carbon nanotubes on human HEK293 cells. Toxicology letters. 2005;155:73-85.

Dhanasekaran M, Uthayathas S, Karuppagounder SS, Parameshwaran K, Suppiramaniam V, Ebadi M, et al. Ebselen effects on MPTP-induced neurotoxicity. Brain Research. 2006;1118:251-4.

Dickey RW, Dickhoff WW. Dispersant and seafood safty. Assessment of potential impacts of COREXIT oil dispersants on seafood safety. . 2011.

Edinger AL, Thompson CB. Death by design: apoptosis, necrosis and autophagy. Current Opinion in Cell Biology. 2004;16:663-9.

Ekwall B. Screening of toxic compounds in mammalian cell cultures. Annals of the New York Academy of Sciences. 1983;407:64-77.

Ekwall B, Silano V, Stammati AP, Zucco F. Toxicity Tests with Mammalian Cell Cultures. In: al PBe, editor. Short-term Toxicity Tests for Non-genotoxic Effects. John Wiley & Sons Ltd1990.

EPA. EPA Response to BP Spill in the Gulf of Mexico. 2010.

EPA EPA. BP Analysis of Subsurface Dispersant Use. 2010.

Fuller C, Bonner J, Page C, Ernest A, McDonald T, McDonald S. Comparative toxicity of oil, dispersant, and oil plus dispersant to several marine species. Environmental Toxicology and Chemistry. 2004;23:2941-9.

Funk D, Schrenk HH, Frei E. Serum albumin leads to false-positive results in the XTT and the MTT assay. Biotechniques. 2007;43.

George-Ares A, Clark J. Aquatic toxicity of two Corexit< sup>®</sup> dispersants. Chemosphere. 2000;40:897-906.

George-Ares A, Clark JR. Aquatic toxicity of two Corexit® dispersants. Chemosphere. 2000;40:897-906.

Gohlke JM, Doke D, Tipre M, Leader M, Fitzgerald T. A review of seafood safety after the deepwater horizon blowout. Environ Health Perspect. 2011;119:1062-9.

Goldstein BD, Osofsky HJ, Lichtveld MY. The Gulf Oil Spill. New England Journal of Medicine. 2011;364:1334-48.

Graham WM, Condon RH, Carmichael RH, D'Ambra I, Patterson HK, Linn LJ, et al. Oil carbon entered the coastal planktonic food web during the Deepwater Horizon oil spill. Environmental Research Letters. 2010;5:045301.

Green DR, Reed JC. Mitochondria and apoptosis. SCIENCE-NEW YORK THEN WASHINGTON-. 1998:1309-12.

Gülden M, Dierickx P, Seibert H. Validation of a prediction model for estimating serum concentrations of chemicals which are equivalent to toxic concentrations in vitro. Toxicology in Vitro. 2006;20:1114-24.

Gulden M, Seibert H. In vitro-in vivo extrapolation: estimation of human serum concentrations of chemicals equivalent to cytotoxic concentrations in vitro. Toxicology. 2003;189:211-22.

Gülden M, Seibert H. Impact of bioavailability on the correlation between in vitro cytotoxic and in vivo acute fish toxic concentrations of chemicals. Aquatic toxicology. 2005;72:327-37.

Gunness P, Aleksa K, Kosuge K, Ito S, Koren G. Comparison of the novel HK-2 human renal proximal tubular cell line with the standard LLC-PK1 cell line in studying drug-induced nephrotoxicity. Can J Physiol Pharmacol. 2010;88:448-55.

Halliwell B, Chirico S. Lipid peroxidation: Its mechanism, measurement, and significance. The American journal of clinical nutrition. 1993;57:715S-24S.

Hayworth JS, Clement TP. BP's Operation Deep Clean—Could Dilution be the Solution to Beach Pollution? Environ Sci Technol. 2011;45:4201-2.

Hayworth JS, Clement TP. Provenance of Corexit-related chemical constituents found in nearshore and inland Gulf Coast waters. Mar Pollut Bull. 2012;64:2005-14.

Hayworth JS, Clement TP, Valentine JF. Deepwater Horizon oil spill impacts on Alabama beaches. Hydrology and Earth System Sciences. 2011;8:15.

Hayworth JS, Clement, T. P., and Valentine, J. F. Deepwater Horizon oil spill impacts on Alabama beaches. Hydrol Earth Syst Sci. 2011;15.

Hazen TC, Dubinsky EA, DeSantis TZ, Andersen GL, Piceno YM, Singh N, et al. Deep-Sea Oil Plume Enriches Indigenous Oil-Degrading Bacteria. Science. 2010;330:204-8.

Hemmer MJ, Barron, M. G. and Greene, R. M. Comparative toxicity of eight oil dispersants, Louisiana sweet crude oil (LSC), and chemically dispersed LSC to two aquatic test species. . Environmental Toxicology and Chemistry. 2011;30:2244–52.

Honma S, Saito M, Kikuchi H, Saito Y, Oshima Y, Nakahata N, et al. A reduction of epidermal growth factor receptor is involved in brefelamide-induced inhibition of phosphorylation of ERK in human astrocytoma cells. European Journal of Pharmacology. 2009;616:38-42.

J. Steven Picou DAG, Christopher L. Dyer, and Evans W. Curry. Disruption and stress in an Alaskan fishing community: initial and continuing impacts of the Exxon Valdez oil spill. Organization & Environment. 1992;6:235-57.

JAG JAG. Review of Preliminary Data to Examine Oxygen Levels in the Vincinity of MC252#1. 2010.

JAG JAG. Review of R/V Brooks McCall Data to Examine Subsurface Oil. 2012.

Jeong B-C, Kwak C, Cho KS, Kim BS, Hong SK, Kim J-I, et al. Apoptosis induced by oxalate in human renal tubular epithelial HK-2 cells. Urological research. 2005;33:87-92.

Judson RS, Martin MT, Reif DM, Houck KA, Knudsen TB, Rotroff DM, et al. Analysis of Eight Oil Spill Dispersants Using Rapid, In Vitro Tests for Endocrine and Other Biological Activity. Environmental Science & Technology. 2010;44:5979-85.

Judson RS, Martin MT, Reif DM, Houck KA, Knudsen TB, Rotroff DM, et al. Analysis of eight oil spill dispersants using rapid, in vitro tests for endocrine and other biological activity. Environ Sci Technol. 2010;44:5979-85.

Kirkpatrick D, Dale K, Catania J, Gandolfi A. Low-level arsenite causes accumulation of ubiquitinated proteins in rabbit renal cortical slices and HEK293 cells. Toxicology and applied pharmacology. 2003;186:101-9.

Kruse PFJ. Tissue Culture: Methods and Applications: Elsevier Science; 1973.

Kujawinski EB, Kido Soule MC, Valentine DL, Boysen AK, Longnecker K, Redmond MC. Fate of dispersants associated with the Deepwater Horizon oil spill. Environmental Science & Technology. 2011;45:1298-306.

Lawal AO, Ellis EM. The chemopreventive effects of aged garlic extract against cadmium-induced toxicity. Environmental Toxicology and Pharmacology. 2011;32:266-74.

Lee K, Wong C, Cretney W, Whitney F, Parsons T, Lalli C, et al. Microbial response to crude oil and Corexit 9527: SEAFLUXES enclosure study. Microbial ecology. 1985;11:337-51.

Lee S, Kim Y-J, Kwon S, Lee Y, Choi SY, Park J, et al. Inhibitory effects of flavonoids on TNF-alpha-induced IL-8 gene expression in HEK 293 cells. BMB Rep. 2009;42:265-70.

Lehr B, Bristol S, Possolo A. Oil Budget Calculator Deepwater Horizon, Technical Documentation, A Report to the National Incident Command, November 2010 (Coastal Response Research Center, University of New Hampshire, Durham, NH). 2010.

Liou S. About Abnormalities in Energy Metabolism. Abnormalities in energy metabolism. 2011.

Lönning S, Hagström BE. Deleterious effects of Corexit 9527 on fertilization and development. Marine Pollution Bulletin. 1976;7:124-7.

Lu T, Finkel T. Free radicals and senescence. Exp Cell Res. 2008;314:1918-22.

Lubchenco J, McNutt MK, Dreyfus G, Murawski SA, Kennedy DM, Anastas PT, et al. Science in support of the Deepwater Horizon response. Proceedings of the National Academy of Sciences. 2012;109:20212-21.

Lustgarten A. Chemicals meant to break up BP Oil spill present new environmental concerns. 2010.

Major D, Zhang Q, Wang G, Wang H. Oil-dispersant mixtures: understanding chemical composition and its relation to human toxicity. Toxicological & Environmental Chemistry. 2012;94:1832-45.

McKim JM, Jr. Building a tiered approach to in vitro predictive toxicity screening: a focus on assays with in vivo relevance. Comb Chem High Throughput Screen. 2010;13:188-206.

Milinkovitch T, Lucas J, Le Floch S, Thomas-Guyon H, Lefrançois C. Effect of dispersed crude oil exposure upon the aerobic metabolic scope in juvenile golden grey mullet (Liza aurata). Marine Pollution Bulletin. 2012;64:865-71.

Min YK, Park JH, Chong SA, Kim YS, Ahn YS, Seo JT, et al. Pyrrolidine dithiocarbamate-induced neuronal cell death is mediated by Akt, casein kinase 2, c-Jun N-terminal kinase, and IκB kinase in embryonic hippocampal progenitor cells. Journal of Neuroscience Research. 2003;71:689-700.

Mitchell FM, Holdway DA. The acute and chronic toxicity of the dispersants Corexit 9527 and 9500, water accommodated fraction (WAF) of crude oil, and dispersant enhanced WAF (DEWAF) to< i> Hydra viridissima</i>(green hydra). Water Research. 2000;34:343-8.

Morrione A, Romano G, Navarro M, Reiss K, Valentinis B, Dews M, et al. Insulin-like growth factor I receptor signaling in differentiation of neuronal H19-7 cells. Cancer research. 2000;60:2263-72.

Mosmann T. Rapid colorimetric assay for cellular growth and survival: Application to proliferation and cytotoxicity assays. J Immunol Methods. 1983;65:55-63.

Mulligan JM, Campiani G, Ramunno A, Nacci V, Zisterer DM. Inhibition of G1 cyclin-dependent kinase activity during growth arrest of human astrocytoma cells by the pyrrolo-1,5-benzoxazepine, PBOX-21. Biochimica et Biophysica Acta (BBA) - Molecular Basis of Disease. 2003;1639:43-52.

Myers DG. Exploring Psychology in Modules 2013.

Mytilineou C, Kramer BC, Yabut JA. Glutathione depletion and oxidative stress. Parkinsonism Relat Disord. 2002;8:385-7.

NALCO. Materal Safety Data Sheet 2010.

NIH NIoH. Household Products Database. 2013.

NRC NRC. Using Oil Spill Dispersant on the Sea. Washington, D.C.: National Academy Press; 1989.

NRC NRC. Oil in the Sea III: Inputs, Fates, and Effects. 2003.

NRC NRC. Oil Spill in the Sea: Inputs, Fates and Effects. National Academic Press, Washington, DC. 2003.

NRC NRC. Oil Spill Dispersants: Efficacy and Effects. . http://www.hap.edu/catalog/11283.html2005.

Ohkawa H, Ohishi N, Yagi K. Assay for lipid peroxides in animal tissues by thiobarbituric acid reaction. Analytical biochemistry. 1979;95:351-8.

OSTA OSAT. Summary report for fate and effects of remnant oil in the beach environment. 2011.

Pan M, Han H, Zhong C, Geng Q. Effects of genistein and daidzein on hippocampus neuronal cell proliferation and BDNF expression in H19-7 neural cell line. The journal of nutrition, health & aging. 2012;16:389-94.

Passos JF, Von Zglinicki T. Oxygen free radicals in cell senescence: are they signal transducers? Free Radic Res. 2006;40:1277-83.

Peraza M, Carter D, Gandolfi A. Toxicity and metabolism of subcytotoxic inorganic arsenic in human renal proximal tubule epithelial cells (HK-2). Cell biology and toxicology. 2003;19:253-64.

Pitkanen S, Robinson BH. Mitochondrial complex I deficiency leads to increased production of superoxide radicals and induction of superoxide dismutase. Journal of Clinical Investigation. 1996;98:345.

PontÉN JAN, Macintyre EH. LONG TERM CULTURE OF NORMAL AND NEOPLASTIC HUMAN GLIA. Acta Pathologica Microbiologica Scandinavica. 1968;74:465-86.

QARAWI MA, CARRINGTON S, BLAGBROUGH IS, MOSS SH, POUTON CW. Optimization of the MTT assay for B16 murine melanoma cells and its application in assessing growth inhibition by polyamines and novel polyamine conjugates. Pharmacy and Pharmacology Communications. 1997;3:235-9.

Rapoport R, Hanukoglu I, Sklan D. A fluorimetric assay for hydrogen peroxide, suitable for NAD(P)H-dependent superoxide generating redox systems. Anal Biochem. 1994;218:309-13.

Rick A. Flurer, Brian L B, Bryan Gamble, Samuel Gratz, Mulligan KJ. Determination of dioctylsulfosuccinate in select seafoods using a quechers extraction with liquid chromotography-triple quadrupole mass spectrometry 2010.

Rico-Martínez R, Snell TW, Shearer TL. Synergistic toxicity of Macondo crude oil and dispersant Corexit 9500A® to the Brachionus plicatilis species complex (Rotifera). Environmental Pollution. 2013;173:5-10.

Roberts JR, Reynolds JS, Thompson JA, Zaccone EJ, Shimko MJ, Goldsmith WT, et al. Pulmonary Effects after Acute Inhalation of Oil Dispersant (COREXIT EC9500A) in Rats. Journal of Toxicology and Environmental Health, Part A. 2011;74:1381-96.

Sakon S, Xue X, Takekawa M, Sasazuki T, Okazaki T, Kojima Y, et al. NF-κB inhibits TNF-induced accumulation of ROS that mediate prolonged MAPK activation and necrotic cell death. The EMBO journal. 2003;22:3898-909.

Samuel Gratz, Angela Mohrhaus, Bryan Gamble, Jill Gracie, David Jackson, John Roetting, et al. Screen for the presence of polycyclic aromatic hydrocarbons in select seafoods using LC-Fluorescence. Laboratory Information Bulletin. 2010.

Sato T, Hashizume M, Hotta Y, Okahata Y. Morphology and proliferation of B16 melanoma cells in the presence of lanthanoid and Al3+ ions. Biometals. 1998;11:107-12.

Schulze-Osthoff K, Beyaert R, Vandevoorde V, Haegeman G, Fiers W. Depletion of the mitochondrial electron transport abrogates the cytotoxic and gene-inductive effects of TNF. The EMBO journal. 1993;12:3095.

Seibert H, Kolossa M, Wassermann O. Bovine spermatozoa as anin vitro model for studies on the cytotoxicity of chemicals: effects of chlorophenols. Cell biology and toxicology. 1989;5:315-30.

Shaw G, Morse S, Ararat M, Graham FL. Preferential transformation of human neuronal cells by human adenoviruses and the origin of HEK 293 cells. Faseb J. 2002;16:869-71.

Shimohama S. Apoptosis in Alzheimer's disease--an update. Apoptosis. 2000;5:9-16.

Shirahata S, Kabayama S, Nakano M, Miura T, Kusumoto K, Gotoh M, et al. Electrolyzed–Reduced Water Scavenges Active Oxygen Species and Protects DNA from Oxidative Damage. Biochemical and Biophysical Research Communications. 1997;234:269-74.

Shu B, Duan W, Yao J, Huang J, Jiang Z, Zhang L. Caspase 3 is involved in the apoptosis induced by triptolide in HK-2 cells. Toxicology in Vitro. 2009;23:598-602.

Simon H-U, Haj-Yehia A, Levi-Schaffer F. Role of reactive oxygen species (ROS) in apoptosis induction. Apoptosis. 2000;5:415-8.

Simon HU, Haj-Yehia A, Levi-Schaffer F. Role of reactive oxygen species (ROS) in apoptosis induction. Apoptosis. 2000;5:415-8.

Singer M, Aurand D, Bragin G, Clark J, Coelho G, Sowby M, et al. Standardization of the preparation and quantitation of water-accommodated fractions of petroleum for toxicity testing. Marine Pollution Bulletin. 2000;40:1007-16.

Singer MM, George S, Benner D, Jacobson S, Tjeerdema RS, Sowby ML. Comparative toxicity of two oil dispersants to the early life stages of two marine species. Environmental Toxicology and Chemistry. 1993;12:1855-63.

Singer MM, George S, Jacobson S, Lee I, Weetman LL, Tjeerdema RS, et al. Comparison of acute aquatic effects of the oil dispersant Corexit 9500 with those of other Corexit series dispersants. Ecotoxicology and Environmental Safety. 1996;35:183-9.

Southward A, Southward EC. Recolonization of rocky shores in Cornwall after use of toxic dispersants to clean up the Torrey Canyon spill. Journal of the Fisheries Board of Canada. 1978;35:682-706.

Southward AJ, Southward EC. Recolonization of Rocky Shores in Cornwall After Use of Toxic Dispersants to Clean Up the Torrey Canyon Spill. Journal of the Fisheries Research Board of Canada. 1978;35:682-706.

Sriram K, Lin GX, Jefferson AM, Goldsmith WT, Jackson M, McKinney W, et al. Neurotoxicity following acute inhalation exposure to the oil dispersant COREXIT EC9500A. J Toxicol Environ Health A. 2011;74:1405-18.

Stacey G, Viviani B. Cell culture models for neurotoxicology. Cell biology and toxicology. 2001;17:319-34.

Sung JY, Kim J, Paik SR, Park JH, Ahn YS, Chung KC. Induction of neuronal cell death by Rab5A-dependent endocytosis of α-synuclein. Journal of Biological Chemistry. 2001;276:27441-8.

Turrens JF. Superoxide production by the mitochondrial respiratory chain. Bioscience reports. 1997;17:3-8.

Twentyman P, Luscombe M. A study of some variables in a tetrazolium dye (MTT) based assay for cell growth and chemosensitivity. British journal of cancer. 1987;56:279.

UCBerkeley. National Commission on the BP Deepwater Horizon Oil Spill and Offshore Drilling. 2010.

Vistica DT, Skehan P, Scudiero D, Monks A, Pittman A, Boyd MR. Tetrazolium-based assays for cellular viability: a critical examination of selected parameters affecting formazan production. Cancer research. 1991;51:2515-20.

Wallace DC, Melov S. Radicals r'aging. Nature genetics. 1998;19:105-6.

Wan S, Izzat MB, Lee TW, Wan IYP, Tang NLS, Yim APC. Avoiding cardiopulmonary bypass in multivessel CABG reduces cytokine response and myocardial injury. The Annals of Thoracic Surgery. 1999;68:52-6.

Wang C, Wu X, Chen M, Duan W, Sun L, Yan M, et al. Emodin induces apoptosis through caspase 3-dependent pathway in HK-2 cells. Toxicology. 2007;231:120-8.

Wang H, Shi Y, Major D, Yang Z. Lung epithelial cell death induced by oil-dispersant mixtures. Toxicology in Vitro. 2012;26:746-51.

Wardrop J, Butler A, Johnson J. A field study of the toxicity of two oils and a dispersant to the mangrove Avicennia marina. Mar Biol. 1987;96:151-6.

Wikipedia. Dispersant. 2010.

Wilk A, Waligórski P, Lassak A, Vashistha H, Lirette D, Tate D, et al. Polycyclic aromatic hydrocarbons - induced ROS accumulation enhances mutagenic potential of T-antigen from human polyomavirus JC. Journal of Cellular Physiology. 2013:n/a-n/a.

Winterbourn CC. Toxicity of iron and hydrogen peroxide: the Fenton reaction. Toxicology letters. 1995;82:969-74.

Woiniak A, Drewa G, Wozniak B, Schachtschabel DO, Mila-Kierzenkowska C, Drewa T, et al. The effect of antitumor drugs on oxidative stress in B16 and S91 melanoma cells in vitro. Med Sci Monit. 2005;11:BR22-9.

Ye Y, Chu J-H, Wang H, Xu H, Chou G-X, Leung AK-M, et al. Involvement of p38 MAPK signaling pathway in the anti-melanogenic effect of San-bai-tang, a Chinese herbal formula, in B16 cells. Journal of Ethnopharmacology. 2010;132:533-5.

Zhang ZD, Cox G. MTT assay overestimates human airway smooth muscle cell number in culture. Biochem Mol Biol Int. 1996;38:431-6.